Inorg. Chem. **2002**, *41*, 5986–6000

Synthesis and Characterization of Diametrically Substituted Tetra-*O*-*n*-butylcalix[4]arene Ligands and Their Chelated Complexes of Titanium, Molybdenum, and Palladium

Daniel R. Evans,*,† Mingsheng Huang,† James C. Fettinger,† and Tracie L. Williams‡

Department of Chemistry and Biochemistry, University of Maryland, College Park, Maryland 20742, and U.S. Food and Drug Administration, Center for Food Safety and Nutrition, College Park, Maryland 20741

Received July 9, 2002

The ligation properties of three new upper-rim-substituted calix[4]arene ligands, 5,17-bis(hydroxymethyl)-tetra-*n*-butoxycalix[4]arene ($(HOCH_2)_2$-^{n}Bu_4Clx, **7**), 5,17-bis((diphenylphosphinito)methoxy)-tetra-*n*-butoxycalix[4]arene ($(PPh_2OCH_2)_2$-^{n}Bu_4Clx, **8**), and 5,17-bis((diphenylphosphino)methyl)-tetra-*n*-butoxycalix[4]arene ($(PPh_2CH_2)_2$-^{n}Bu_4Clx, **10**) are reported herein. The newly prepared compounds differ from previously reported diametrically substituted calix[4]arene derivatives in that the lower-rim substituent was *n*-butyl. The presence of this lower-rim substituent did not reduce the inherent crystallinity of these complexes as purification of all materials occurred via simple crystallizations. The key precursor for the syntheses of **8** and **10** was **7**, acquisition of which occurred in six steps starting from tetra-*tert*-butylcalix[4]arene, **1**. Calix[4]arene derivatives include, tetra-*n*-butoxycalix[4]arene (^{n}Bu_4Clx, **3**), 5,11,17,23-tetrabromo-tetra-*n*-butoxycalix[4]arene (Br_4-^{n}Bu_4Clx, **4**), 5,17-dibromo-tetra-*n*-butoxycalix[4]arene (Br_2-^{n}Bu_4Clx, **5**), 5,17-bis(formyl)-tetra-*n*-butoxycalix[4]arene ($(CHO)_2$-^{n}Bu_4Clx, **6**), and 5,17-bis(chloromethyl)-tetra-*n*-butoxycalix[4]arene ($(ClCH_2)_2$-^{n}Bu_4Clx, **9**), all of which were synthesized using modifications of existing procedures. Characterization of all compounds occurred, when possible, using ^{1}H, ^{13}C, and ^{31}P NMR, elemental analyses, FAB-MS, ESI-MS, FT-IR, and X-ray crystallography. The solid-state structures of all calix[4]arene intermediates and ligands showed that the annulus adopted the pinched-cone conformation in which the average C(5)···C(17) intraannular separation was 4.5 ± 0.4 Å. Reaction of **7** with $CpTiMe_3$ yielded the cis-chelate, CpTi(Me)[$(OCH_2)_2$-^{n}Bu_4Clx] (**11**), quantitatively. Data obtained using ESI-MS (positive-ion mode) confirmed the monomer formulation showed above, and ^{1}H NMR spectra provided sufficient information to deduce the nature of the Ti coordination sphere. Reaction of **8** with *cis*-$Cl_2Pd(NCPh)_2$ in refluxing benzene afforded *cis*-$Cl_2Pd[(PPh_2OCH_2)_2$-^{n}Bu_4Clx] (**12**) in good yields. The monomeric identity of this compound was verified by both X-ray crystallography and positive-ion ESI-MS. The cis-bidentate calix[4]arene ligand did not undergo any noticeable contortion upon chelation of the $PdCl_2$ fragment. Acid-promoted decomposition of **12** occurred in the presence of adventitious HCl and gaseous HCl, and the products of this decomposition were **9** and [μ_2-ClPd$(PPh_2OH)(PPh_2O)]_2$. In addition, chelates of **8** that contained $Mo(CO)_3$L (L = NCMe (**14a**), NCEt (**14b**), and CO (**14c**)) showed that the mode of coordination was relatively insensitive to the identity of the metal. X-ray crystallography afforded views of the solid-state structures of **14b,c** and, like **12**, showed that the $Mo(CO)_3$L fragment resided above the pinched-cone of the calix[4]arene. ^{1}H NMR revealed that C–H/π interactions existed between L (**14a,b**) and a phenyl ring of the coordinated phosphinite. Finally, the bis(diphenylphosphine)calix[4]arene ligand (**10**) readily coordinated the $Mo(CO)_3$L species, but the reaction did not go to completion, as evidenced by ^{1}H NMR, even after a 5 day reaction time. Data suggest that the product is similar to that observed for **12** and **14**, but the incomplete reaction complicated attempts to obtain pure material and prohibited definitive assignment of the coordination array.

Introduction

Calix[4]arenes are host molecules that possess a tetragonal array of phenolic rings joined by methylene linkers, Chart 1.[1] This arrangement is attractive in that functionalization of the lower-rim phenolic oxygens with alkyl chains, R > ^{n}Pr, enforces the cone-shaped structure of the molecule, while

* To whom correspondence should be addressed. E-mail: de44@umail.umd.edu.
† University of Maryland.
‡ U.S. Food and Drug Administration.

(1) (a) Gutsche, C. D. In *Calixarenes*, 1st ed.; The Royal Society of Chemistry: Cambridge, U.K., 1989. (b) Gutsche, C. D. In *Calixarenes Revisited*, 1st ed.; The Royal Society of Chemistry: Cambridge, U.K., 1998. (c) Gutsche, C. D. *Aldrichim. Acta* **1995**, *28*, 3−10.

10.1021/ic020446b CCC: $22.00
Published on Web 10/15/2002

Chart 1

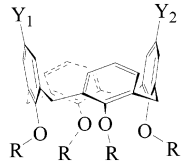

the introduction of ligating elements, Y, on the upper-rim provides an opportunity to introduce transition metals above the annulus of the calix[4]arene.[2] This aspect makes this class of compounds particularly fascinating, as it is easy to envision that this class of compounds could be used to (i) create catalytic systems with greater selectivity,[3] (ii) generate small-molecule[4] or anion sensors,[5] (iii) serve as effective cationic lanthanide extraction agents,[6] and (iv) provide an enthalpic trap that would promote the formation of alkane−metal complexes. While examples ii and iii now exist, it is still unclear whether these species will be able to affect selectivity in catalytic processes or have a cavity large enough to encapsulate alkanes. Considering the potential utility of this class of ligands to a number of diverse areas in inorganic chemistry, it is of importance to highlight some recently recognized features and coordination properties.

The desire to exploit the presence of a hydrophobic pocket in these types of molecules requires the recognition of a potential drawback—functionalization of the lower-rim oxygens. This synthetic modification is a necessary prerequisite as the parent calix[4]arenes, R = H, are capable of adopting three different conformations.[1] Unfortunately, the process of tetra-O-alkylation gives rise to a molecule that adopts a pinched-cone conformation, in which there is a substantial reduction of the effective volume of the cavity when compared to the underivatized species. Synthetic strategies are available that promote an enlargement of the size of the cavity (cf. refs 4 and 5), but increasingly complicated routes result in a reduction of the amount of material in hand.

Another challenging aspect is prediction of the mode of coordination and the presence or absence of a hydrophobic pocket. For example, calix[4]arene ligands ($Y_1 = Y_2 = PPh_2$, R = ^{n}Pr,[7a,c] R = Bz[7b]) participate in either cis or trans metal ligation in which monomers and dimers are possible.[7] In the case of the monomeric species (M = Ru(II), Pt(II)), trans-ligation resulted in a slight expansion of the cavity relative to free ligand,[7a,b] but cis adducts (M = Pd(II), Pt(II)) provided a metal fragment that resided over a hydrophobic cleft, made available by the splayed arenes.[7b,c] Species that possess a single phosphine ligand ($Y_1 = PPh_2$, Y_2=H,[8] Y_2 = H/Br[7c]) coordinate either Rh(III) or Ru(II) in strikingly different ways.[7c,8] In the former case,[8] the ligand directed the metal fragment (Cp^*Cl_2Rh) away from the pinched-cone, but in the latter, the (*p*-cymene)Cl_2Ru arrangement resided above the cavity in which encapsulation of the η^6-*p*-cymene occurred within the confines of the cavity.[7c] A variation of the above-mentioned ligand is to include linkers (either Y = $-CH_2PPh_2$ or Y = $-CH_2OPR_2$) between the upper rim of the cavity and the P-type ligand.[9] Species that contain a single methylene spacer ($Y_1 = Y_2 = -CH_2PPh_2$),[9a,b] do not readily chelate metals above the open mouth of the cavity but instead give rise to polymeric products. This is in contrast to a calix[4]arene that contains the methyleneoxo ($-CH_2O-$) spacer.[9a] A single report described the coordination chemistry of this type of bidentate ligand, and ^{1}H NMR provided sufficient data to allow the authors to correctly deduce the coordination geometry. At the onset of this work, the variety of coordination modes was hard to predict, but with recent reports and the data presented herein, a more lucid picture is slowly emerging.

An understanding of how to introduce metals above an opened cavity of the calix[4]arene molecule is crucial to one aspect of our research program.[10] This entails the utilization of these basket-containing molecules to explore the final frontier of coordination chemistry, i.e., the interactions that occur between alkanes and metals. Our interest in this area came from the fortuitous discovery of an alkane−metal complex.[11] This report showed that the host properties of a porphyrin array served to encapsulate a heptane molecule in the immediate vicinity of a coordinatively unsaturated Fe(II) center. Complete characterization of this interaction was fraught with difficulties, as the complex was insoluble in hydrocarbon solvents, thereby prohibiting the possibility of solution-phase NMR spectroscopic analysis. It seemed logical to devise systems that contained a metal fragment in close proximity to a cavity-containing molecule, with the caveat that they possess solubility in hydrocarbon solvents.

(2) Wieser, C.; Dieleman, C. B.; Matt, D. *Coord. Chem. Rev.* **1997**, *165*, 93−161.
(3) (a) Shimizu, S.; Shirakawa, S.; Sasaki, Y.; Hirai, C. *Angew. Chem., Int. Ed.* **2000**, *39*, 1256−1259. (b) Cobley, C. J.; Ellis, D. D.; Orpen, A. G.; Pring, P. G. *J. Chem. Soc., Dalton Trans.* **2000**, 1109−1112. (c) Parlevliet, F. J.; Kiener, C.; Fraanje, J.; Goubitz, K.; Lutz, M.; Spek, A. L.; Kamer, P. C. J.; van Leeuwen, P. W. N. M. *J. Chem. Soc., Dalton Trans.* **2000**, 1113−1122.
(4) (a) Cameron, B. R.; Loeb, S. J. *Chem. Commun.* **1996**, 2003−2004. (b) Cameron, B. R.; Loeb, S. J.; Yap, G. P. A. *Inorg. Chem.* **1997**, *36*, 5498−5504.
(5) (a) Beer, P. D.; Hesek, D.; Kingston, J. E.; Smith, D. K.; Stokes, S. E.; Drew, M. G. B. *Organometallics* **1995**, *14*, 3288−3295. (b) Szemes, F.; Hesek, D.; Chen, Z.; Dent, S. W.; Drew, M. G. B.; Goulden, A. J.; Graydon, A. R.; Grieve, A.; Mortimer, R. J.; Wear, T.; Weightman, J. S.; Beer, P. D. *Inorg. Chem.* **1996**, *35*, 5868−5879. (c) Beer, P. D.; Hesek, D.; Nam, K. C.; Drew, M. G. B. *Organometallics* **1999**, *18*, 3933−3943.
(6) (a) Delmau, L. H.; Simon, N.; Schwing-Weill, M.-J.; Arnaud-Neu, F.; Dozol, J.-F.; Eymard, S.; Tournois, B.; Bohmer, V.; Gruttner, C.; Musigmann, C.; Tunayar, A. *Chem. Commun.* **1998**, 1627−1628. (b) Lambert, B.; Jacques, V.; Shivanyuk, A.; Matthews, S. E.; Tunayar, A.; Baaden, M.; Wipff, G.; Bohmer, V.; Desreux, J. F. *Inorg. Chem.* **2000**, *39*, 2033−2041.
(7) (a) Wieser-Jeunesse, C.; Matt, D.; De Cian, A. *Angew. Chem., Int. Ed.* **1998**, *37*, 2861−2864. (b) Takenaka, K.; Obora, Y.; Jiang, L. H.; Tsuji, Y. *Organometallics* **2002**, *21*, 1158−1166. (c) Lejeune, M.; Jeunesse, C.; Matt, D.; Kyritsakas, N.; Welter, R.; Kintzinger, J.-P. *J. Chem. Soc., Dalton Trans.* **2002**, 1642−1650.
(8) (a) Vezina, M.; Gagnon, J.; Villeneuve, K.; Drouin, M.; Harvey, P. D. *Chem. Commun.* **2000**, 1073−1074. (b) Vezina, M.; Gagnon, J.; Villeneuve, K.; Drouin, M.; Harvey, P. D. *Organometallics* **2001**, *20*, 273−281.
(9) (a) Bagatin, I. A.; Matt, D.; Thonnessen, H.; Jones, P. G. *Inorg. Chem.* **1999**, *38*, 1585−1591. (b) Fang, X.; Scott, B. L.; Watkin, J. G.; Carter, C. A. G.; Kubas, G. J. *Inorg. Chim. Acta* **2001**, *317*, 276−281.
(10) (a) Evans, D. R.; Huang, M.; Seganish, W. M.; Fettinger, J. C.; Williams, T. L. *Organometallics* **2002**, *21*, 893−900. (b) Evans, D. R.; Huang, M.; Seganish, W. M.; Chege, E. W.; Fettinger, J. C.; Lam, Y.-F.; Williams, T. L. *Inorg. Chem.* **2002**, *41*, 2633−2641.
(11) Evans, D. R.; Drovetskaya, T.; Bau, R.; Reed, C. A.; Boyd, P. W. D. *J. Am. Chem. Soc.* **1997**, *119*, 3633−3643.

Scheme 1 [a]

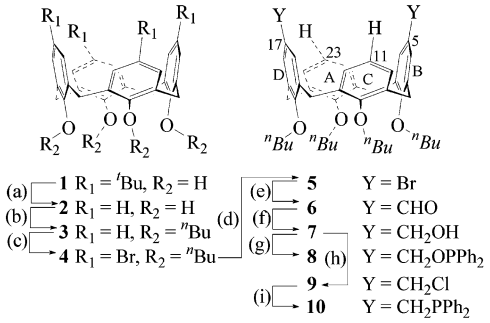

[a] Legend: (a) (2) **1** + $AlCl_3$ (1:4.8), in toluene, 55 °C, 2 h; (b) (**3**) **2** + (i) NaH (1:4), (ii) xs ^{n}BuBr, in DMF, 80 °C, 6 h; (c) (**4**) **3** + NBS (1:6:6), acetone, 25 °C, 12 h; (d) (**5**) **4** (i) ^{n}BuLi (1:2.1), (ii) xs MeOH, in THF, −78 °C; (e) (**6**) **5** + (i) ^{n}BuLi (1:2.1), (ii) DMF in THF, −78 °C; (f) (**7**) **6** + $LiAlH_4$ in Et_2O, 25 °C; (g) (**8**) **7** + (i) pyridine (1:2.2), (ii) Ph_2PCl (1:2.0) in THF, rt, 12 h; (h) (**9**) **7** + $SOCl_2$ (1:2.5) in $CHCl_3$, 22 °C, 4 h; (i) (**10**) **9** + $LiPPh_2$ (1:2) in THF, −78 °C, 2 h.

Ideal candidates to explore with this goal in mind are the metal chelates of 5,17-disubstituted-tetra-O-alkylated calix[4]arenes. The ultimate goal is to fit the cavities with metals in which positions of coordinative unsaturation may be directed toward the interior of the cavity. Ideally, the cavity space will be large enough to encapsulate small alkanes but small enough to exclude larger unwanted molecules.

In an attempt to enter this interesting area of research we have devised a synthetic route, on the basis of existing procedures, for the preparation of upper-rim-functionalized calix[4]arenes capable of ligating metal centers with a propensity to interact with alkanes. While it is difficult to predict nature of metal ligation until it has been achieved, results provided herein serve to confirm expectations that P-type ligands, when separated from the cavity by a $-CH_2O-$ linker, result in cis-chelates. Corroboration of this statement occurred upon the synthesis and characterization of three upper-rim-functionalized calix[4]arene-based ligands that chelated metal fragments composed of Ti(IV), Pd(II), and Mo(0).

Results and Discussion

Preparation and Characterization of Calix[4]arene Ligand Precursors. Several synthetic strategies are presently available for the preparation of diametrically substituted calix[4]arenes.[1b,3a,4,5,7,9] The selected pathway, Scheme 1, showing an abbreviated numbering arrangement,[1] resembles that adopted by Matt et al.,[9a] with the exception that lower-rim functionalization proceeded with *n*-butyl substituents. Utilization of the *n*-butyl groups is advantageous in that they provide additional solubility without a sacrificial loss of crystallinity. Evidence to support this latter point comes from the fact that purification of all synthetic intermediates and ligands occurred via simple crystallizations.

The starting point for the synthesis of these ligands is ^{t}Bu$_4$-Clx, **1**. Preparation of this material from commercially available 4-*tert*-butylphenol is straightforward using a known method.[12] The scale of this protocol was successfully increased by a factor of 3 providing comparable yields. This modification resulted in the acquisition of kilogram quantities of material in a 2-week period. Removal of the upper-rim *tert*-butyl substituents to form Clx, **2**, occurred using a modification of a published procedure.[13] Adoption of a known synthetic step afforded tetra-O-alkylation of the phenolic oxygens that provided ^{n}Bu$_4$-Clx, **3**, in excellent yields.[14] Preparation of the tetrabrominated calix[4]arene, Br$_4$-^{n}Bu$_4$-Clx, **4**, species proceeded at room temperature using NBS and reagent grade acetone.[15] A descriptive process served as a guide for the preparation of the diametrically substituted (C5 and C17, rings B and D, Scheme 1) derivatives **5** and **6**.[16] The synthetic scheme presented for EtOEt$_4$-Clx derivatives[9a] afforded **7**, **9**, and **10**, while synthesis of **8** occurred using an adaptation of a method for the preparation of glucofuranose−phosphinite derivatives.[17] All synthetic intermediates were fully characterized, and the molecular structures for all newly synthesized species, except **9**, were accurately determined. Synthetic and X-ray crystallographic details are available in the Experimental Section and Supporting Information, respectively. Acquisition of high-purity crystalline material afforded elemental analyses in agreement with expectations. The ^{1}H and ^{13}C NMR spectroscopic features of all derivatives and ligands are in close agreement with previously reported tetra- and diametrically substituted R$_4$-Clx derivatives, with the only difference being due to the presence of the *O*-*n*-butyl substituent. Crystallographically determined structures of **3**−**8** and **10** showed that the calix[4]arene cavity possessed the pinched-cone conformation in the solid-state; see Discussion and the Supporting Information.

Metal Chelation with Bidentate Ligands. Bis(alkoxy)-calix[4]arene Complexation. Due to the relative ease in preparing **7**, it served as a springboard for these complexation studies. Alkoxy complexes of group 4 metals are readily available;[18] thus, we chose these metals to explore with this system. For example, **7** reacted immediately with $CpTiMe_3$ in toluene at room temperature to form **11** and methane, eq 1. Despite repeated attempts, this material failed to crystal-

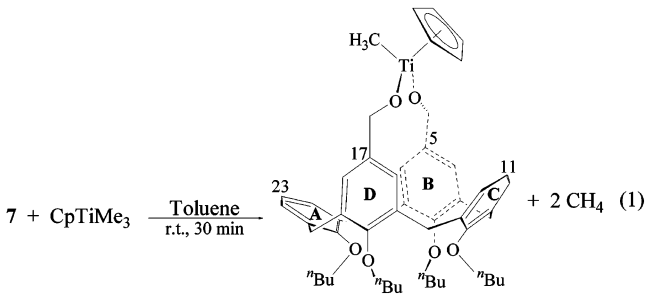

lize, and always existed as an off-white powder. Failure to

(12) Gutsche, C. D.; Iqbal, M. *Org. Synth.* **1990**, *68*, 234−236.

(13) Gutsche, C. D.; Levine, J. A.; Sujeeth, P. K. *J. Org. Chem.* **1985**, *50*, 5802−5806.

(14) Kenis, P. J. A.; Noordman, O. F. J.; Schonherr, H.; Kerver, E. G.; Snellink-Ruel, B. H. M.; van Hummel, G. J.; Harkema, S.; van der Vorst, C. P. J. M.; Hare, J.; Picken, S. J.; Engbersen, J. F. J.; van Hulst, N. F.; Vancso, G. J.; Reinhoudt, D. N. *Chem.—Eur. J.* **1998**, *4*, 1225−1234.

(15) Gutsche, C. D.; Pagoria, P. F. *J. Org. Chem.* **1985**, *50*, 5795−5802.

(16) Larsen, M.; Jorgensen, M. *J. Org. Chem.* **1996**, *61*, 6651−6655.

(17) Johnson, T. H.; Rangarajan, G. *J. Org. Chem.* **1980**, *45*, 62−65.

obtain crystalline material, coupled with its inherent air-sensitivity, resulted in variable microanalytical data. The results obtained by ESI-MS (positive ion mode) confirmed its monomeric identity in solution (**11** − CH_3^+, *m*/*z* 819.4115 amu). Due to the lack of crystallinity, an X-ray structure of this complex was not possible, but analysis of the ^{1}H NMR spectrum provided ample clues as to the nature of the coordination array. The ^{1}H NMR spectrum of **11** is consistent with bidentate ligation about the titanium atom where the bis(alkoxy) ligation is cis, and the CH_3 and Cp ligands reside above different halves of the pinched-cone. ^{1}H NMR showed that the geometry of the coordination sphere gave rise to a reduction of the overall molecular symmetry, as compared to the free ligand. This is evident upon comparison of the ^{1}H NMR spectra of **7** and **11** in C_6D_6, Figure S1 (Supporting Information). Upon chelation, the hydrogens of the C(5) and C(17) methylene substituents go from a singlet at 4.19 ppm (**7**) to an AB quartet (4.89, 4.86 ppm, $^2J_{AB}$ = 12.4 Hz) (**11**). Further inequivalence occurred for the bridging calix[4]arene methylenes, $ArCH_2Ar$, in which normal doublets (AB spin system) for the axial and equatorial hydrogens in **7** gave rise to two sets of doublets. The B and D ring ArH resonances provided an informative glimpse of the symmetry of the complex, as two doublets appeared at 6.45 and 6.41 ppm. The inequivalence of these resonances suggests that the methyl and Cp ligands reside over different halves of the pinched-cone. If the metal adopts a "twisted-conformation" above the mouth of the pinched-cone,[9a] then some dynamic exchange pathway must be present to account for the observed spectroscopic features; see below. The Cp *H* and Ti−CH_3 resonances appeared at 6.03 and 0.8 ppm, respectively.

Reaction of **7** with either $TiCl_4$ or $ZrCl_4$ was attempted, but the results were not promising. The reaction of **7** with either $TiCl_4$ or $ZrCl_4$ in THF/toluene solutions occurred in the presence of 2 equiv of NEt_3. The former reaction products were too numerous to draw any conclusions, but it was evident that metalation occurred due to the formation of the $HNEt_3^+$ salt. The reaction of **7** with $ZrCl_4$ gave rise to a deep purple solution, which upon filtration and subsequent evaporation of the solvent gave a purple crystalline material. ^{1}H NMR spectra of the product mixture provided evidence to suggest that several decomposition pathways of the calix[4]arene ligand were available. The particular route of decomposition was not determined, but detection of **6** by ^{1}H NMR suggested that a β-elimination pathway was available for the Zr−bis(alkoxy)calix[4]arene complex. Another possibility is that cleavage of the butoxy ether groups occurred under these conditions. A recent study provided evidence, obtained by MALDI-TOF-MS, which showed that diametrically substituted tetra-*O*-propoxycalix[4]arenes, 5,17-R_2-^{n}Pr_4Clx, underwent cleavage of the propoxy ether groups in the presence of $ZrCl_4$.[19]

Bis(phosphinito) Complexation. The conversion of **7** to **8** provided ample quantities of the bis(phosphinite) ligand which served as the ligand of choice for this study. The complexation of **8** with *cis*-$Cl_2Pd(NCPh)_2$ occurred rapidly (45 min) in refluxing benzene. Removal of the volatiles under vacuum and subsequent workup gave rise to {*cis*-Cl_2Pd-[$(PPh_2OCH_2)_2$-^{n}Bu_4Clx]} (**12**) in 85% yield (eq 2). Characterization of **12** occurred spectroscopically by ^{1}H, ^{13}C, and ^{31}P NMR, and elemental analysis of crystalline material was in excellent agreement with theory. The monomeric nature of **12** was established both in the solid state (X-ray crystallography) and in solution (CH_2Cl_2, M^+-ESI-MS; **12** − Cl^+, *m*/*z* 1217 amu). (Solutions of **12** in CH_2Cl_2 with added methanol showed, by ESI-MS, that aggregation occurred at high concentrations; i.e., dimers, trimers, and tetramers were present in the spectra but the signal intensities of these aggregates were always minor and disappeared completely upon dilution.) A complete discussion of the NMR spectroscopic features of **12** appears after the description of the molecular structure.

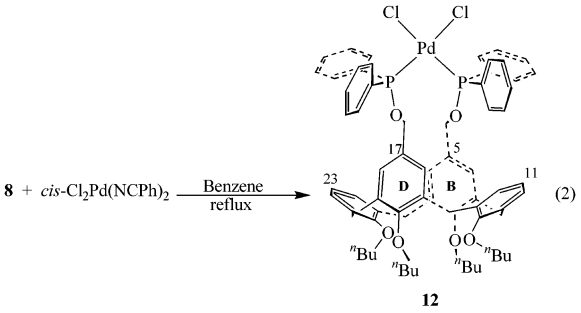

(2)

Figure 1 contains two ORTEP (50% probability) representations of **12**, while Tables 1 and 2 contain selected crystallographic data and metrical parameters, respectively. The view from the side, Figure 1A, shows an abbreviated numbering scheme where the alkyl carbon chains and hydrogens were omitted for clarity. The view from the top, Figure 1B, is somewhat congested but viewable upon omission of the alkyl chains and phosphinitoaryl carbons; several hydrogens (in their calculated positions) are shown. The side view shows that the geometry of the palladium is approximately square planar in which both phosphorus atoms of the $(PPh_2OCH_2)_2$-^{n}Bu_4Clx ligand are cis with P−Pd−P angle of 97.5°. The distances to Pd for both Cl (2.355(5) Å) and P (2.249(6) Å) are remarkably similar to those reported for *cis*-$Cl_2Pd(P(OMe)Ph_2)_2$.[20] The calix[4]arene adopted the pinched-cone conformation as evidenced by the C(5)···C(17) distance of 4.27 Å. An even closer contact of 3.96 Å occurred between the methylene carbons, C(45) and C(58). The view from above, Figure 1B, reveals, ignoring the alkyl chains, a C_2-symmetry element that bisects that Cl−Pd−Cl vertex and passes through the centroid of the calix[4]arene annulus. The least-squares coordination plane is approximately orthogonal to the plane defined by the four arene methylene bridges (C(2), C(8), C(14), and C(20)) with a calculated angle of

(18) Cotton, F. A.; Wilkinson, G. In *Advanced Inorganic Chemistry*, 5th ed.; John-Wiley & Sons: New York, 1988.
(19) Faldt, A.; Kregbs, F. C.; Jorgensen, M. *Tetrahedron Lett.* **2000**, *41*, 1241−1244.
(20) Powell, D. R.; Jacobson, R. A. *Cryst. Struct. Commun.* **1980**, *9*, 1023−1027.

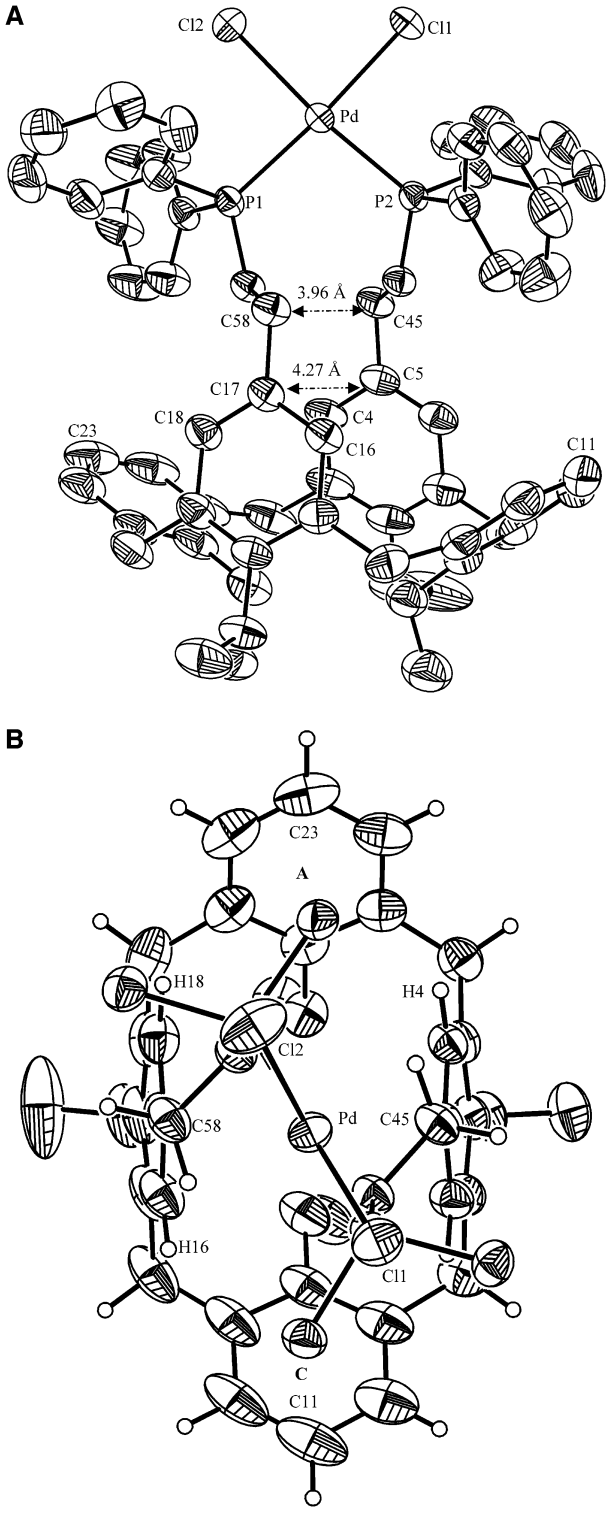

Figure 1. ORTEP representation (50% probability) of *cis*-$Cl_2Pd[(PPh_2\text{-}OCH_2)_2\text{-}^nBu_4Clx]$, **12**: (A) view from the side; (B) view from above. Selected bond distances (Å) and bond angles (deg): Pd(1)−P(2) 2.2452(8), Pd(1)−P(1) 2.2533(8), Pd(1)−Cl(1) 2.3513(9), Pd(1)−Cl(2) 2.3583(8), P(2)−Pd(1)−P(1) 97.46(3), P(2)−Pd(1)−Cl(1) 86.95(3), P(1)−Pd(1)−Cl(1) 175.03(3), P(2)−Pd(1)−Cl(2) 174.09(3), P(1)−Pd(1)−Cl(2) 88.44(3), Cl(1)−Pd(1)−Cl(2) 87.14(3), C(5)···C(17) 4.27. Intraannular distances: C(5)···C(11), 4.27 Å; C(11)···C(23), 10.14 Å. Chloroform solvates, alkyl chains, and hydrogens were omitted for clarity.

90.3°. The mode of coordination observed in **12** is identical to that described for a closely related cationic Pd−calix[4]-arene derivative, $(\eta^3\text{-}C_4H_7)Pd[5,17\text{-}(P(OEt)_2OCH_2)_2\text{-}11,23\text{-}^tBu\text{-}EtOEt_4Clx]^+$.[9a] In this report, the positioning of the coordination plane relative to the annulus of the calix[4]arene pinched-cone was inferred upon inspection of the ^1H NMR spectrum.

Unlike that observed in **11**, the ^1H NMR, in C_6D_6, of **12** did not exhibit an array of inequivalent hydrogens. The hydrogens attached to the B and D rings, H4, H6, H16, and H18, underwent an upfield shift of 0.8 ppm, which is a characteristic signature of these species and is due to the location of these atoms in close proximity to opposing arenes in the pinched-cone conformation.[21] Interestingly, all of the hydrogens appear to be equivalent on the NMR time scale as a single resonance was present, Figure S2. The observation of a singlet for these hydrogens seems to contradict what one might expect upon visualization of the molecular structure of **12**. Close inspection of the top view of **12** shows that H4/H16 and H6/H18 are magnetically inequivalent. In the absence of a dynamic exchange pathway, two singlets should be present for these two sets of hydrogen atoms. The appearance of a singlet indicates the presence of an exchange process that serves to average these hydrogens on the NMR time scale (400.132 MHz); see below.

The common practice of storing NMR solvents over activated 4 Å molecular sieves served to complicate initial solution characterization of **12**. This complex was stable in a number of freshly distilled anhydrous NMR solvents, C_6D_6, C_7D_8, CD_2Cl_2, and $CDCl_3$; however, decomposition of **12** to **9** and a sparingly soluble product occurred in solution while using $CDCl_3$ that was stored over activated molecular sieves. X-ray crystallography provided the means to identify the other product. Identification of this product $[\mu_2\text{-}ClPd(PPh_2\text{-}OH)(PPh_2O)]_2$, **13**, and observation of **9** via ^1H NMR showed that **12** underwent scission of the $-CH_2-O$ bond in the presence of HCl. The minimal stoichiometry for this reaction appears in eq 3, in which the monomer, **12**, while in the presence of HCl, decomposed to **13** and **9**. Confirmation of this decomposition pathway occurred under controlled conditions in which introduction of gaseous HCl to a solution of **12** resulted in the near quantitative recovery of **13**. Characterization of **13** occurred by ^{31}P NMR, elemental analysis, and X-ray crystallography, and identity of **9** was made possible by comparison to authentic material. The ^{31}P NMR spectrum of **13** is nearly identical to that previously reported,[22] and the molecular structure (Figure S11) was virtually indistinguishable from the published structure.[23] This substance crystallized in the crystallographic space group $P2_1/n$, where 1.5 $CHCl_3$'s were present in the lattice. Chloroform solutions of **12** (ca. 5 mM), where the $CHCl_3$ was stored for at least 1 day using zeolite material (activated at 400 °C under vacuo), reproducibly showed complete decomposition within a 24 h period according to eq 3.

(21) Iwamoto, K.; Araki, K.; Shinkai, S. *J. Org. Chem.* **1991**, *56*, 4955−4962.
(22) Wong, E. H.; Bradley, F. C. *Inorg. Chem.* **1981**, *20*, 2333−2335.
(23) Ghaffar, T.; Kieszkiewicz, A.; Nyburg, S. C.; Parkins, A. W. *Acta Crystallogr. C* **1994**, *C50*, 697−700.

Table 1. Crystal Data and Structure Refinement for *cis*-$Cl_2Pd[(PPh_2OCH_2)_2$-$^n Bu_4Clx]$, **12**, and $Mo(CO)_4[(PPh_2OCH_2)_2$-$^n Bu_4Clx]$, **14c**

identificatn code	*cis*-$Cl_2Pd[(PPh_2OCH_2)_2$-$^n Bu_4Clx]$, **12**	$Mo(CO)_4[(PPh_2OCH_2)_2$-$^n Bu_4Clx]$, **14c**
empirical formula	$C_{76}H_{84}O_6P_2Cl_2Pd\cdot 6CHCl_3$	$C_{37}H_{39}O_5PMo\cdot 1/3C_6H_6$
fw	1970.924	1311.35
T (°C)	−80	−100
wavelength (Å)	0.710 73	0.710 73
cryst system	triclinic	trigonal
space group	$P\bar{1}$ (No. 2)	$P\bar{3}c1$ (No. 165)
a (Å)	14.3690(11)	26.166(9)
b (Å)	18.3194(14)	26.166(9)
c (Å)	18.4160(14)	17.935(11)
α (deg)	88.9780(10)	90
β (deg)	71.1410(10)	90
γ (deg)	84.2300(10)	120
V (Å^3)	4563.6(6)	10635(8)
Z	2	3
ρ(calcd) (g/cm^3)	1.434	1.277
μ (mm^{-1})	0.870	0.29
goodness-of-fit on F^2	1.089	1.013
final R[a] indices [$I > 2\sigma(I)$]	$R_1 = 0.0642$, $wR_2 = 0.1997$	$R_1 = 0.0474$, $wR_2 = 0.1220$
R[a] indices (all data)	$R_1 = 0.0795$, $wR_2 = 0.2116$	$R_1 = 0.0645$, $wR_2 = 0.1437$

[a] $R = \Sigma||F_o| - |F_c||/\Sigma|F_o|$; $wR_2 = \{\Sigma[w(F_o^2 - F_c^2)^2]/\Sigma[w(F_o^2)^2]\}^{1/2}$.

Table 2. Selected Bond Lengths (Å) and Angles (deg) for *cis*-$Cl_2Pd[(PPh_2OCH_2)_2$-$^n Bu_4Clx]$, **12**, and $Mo(CO)_4[(PPh_2OCH_2)_2$-$^n Bu_4Clx]$, **14c**

cis-$Cl_2Pd[(PPh_2OCH_2)_2$-$^n Bu_4Clx]$, **12**

Bond Lengths (Å)

Pd(1)−P(2)	2.2452(8)	P(1)−C(46)	1.808(3)
Pd(1)−P(1)	2.2533(8)	P(1)−C(52)	1.816(3)
Pd(1)−Cl(1)	2.3513(9)	P(2)−O(58)	1.607(2)
Pd(1)−Cl(2)	2.3583(8)	P(2)−C(65)	1.808(3)
P(1)−O(45)	1.610(2)	P(2)−C(59)	1.812(3)

Bond Angles (deg)

P(2)−Pd(1)−P(1)	97.46(3)	P(2)−Pd(1)−Cl(2)	174.09(3)
P(2)−Pd(1)−Cl(1)	86.95(3)	P(1)−Pd(1)−Cl(2)	88.44(3)
P(1)−Pd(1)−Cl(1)	175.03(3)	Cl(1)−Pd(1)−Cl(2)	87.14(3)

C···C Intramolecular Distances

C(5)···C(17)	4.27	C(45)···C(58)	3.96
C(11)···C(23)	10.14	C(26)···C(28)	5.32

$Mo(CO)_4[(PPh_2OCH_2)_2$-$^n Bu_4Clx]$, **14c**

Bond Lengths (Å)

Mo(1)−C(3)A	2.013(5)	Mo(1)−P(2)A	2.4910(13)
Mo(1)−C(3)	2.013(5)	Mo(1)−P(2)	2.4910(13)
Mo(1)−C(5)A	2.032(5)	P(2)−O(19)	1.637(3)
Mo(1)−C(5)	2.032(5)		

Bond Angles (deg)

C(5)A−Mo(1)−P(2)	86.43(11)	O(19)−P(2)−C(7)	100.44(16)
C(5)−Mo(1)−P(2)	86.22(11)	O(19)−P(2)−Mo(1)	120.88(10)
P(2)A−Mo(1)−P(2)	100.42(5)	O(4)−C(3)−Mo(1)	174.9(4)
O(19)−P(2)−C(13)	98.27(16)		

C···C Intramolecular Distances

C(5)···C(17)	4.21	C(45)···C(58)	3.74
C(11)···C(23)	10.12	C(26)···C(28)	5.41

Solutions of **12** in $CHCl_3$, where there was no exposure to sieves, were stable over a 3-week period.

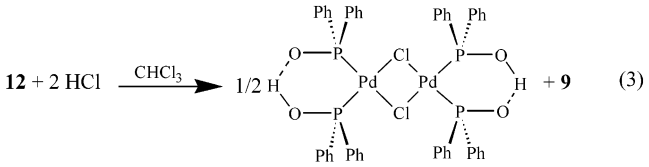

13

The bidentate ligand **8** readily reacted with $Mo(CO)_3$-(toluene) in the presence of either acetonitrile or propionitrile under gentle refluxing conditions within 3 h and yielded the chelated complex in good yields, eq 4. Work up of the residual solid resulted in the isolation of a pale-yellow material with the formulation *fac*-$(CO)_3Mo(L)[(PPh_2OCH_2)$-$^n Bu_4Clx]$ (L = $NCCH_3$, **14a**, L = $NCCH_2CH_3$, **14b**). Both complexes were isolated upon rapid crystallization from benzene solutions. This material was amenable to FT-IR analysis, and elemental analyses provided excellent agreement with theory. Unfortunately, both species were somewhat unstable in solution, though freshly prepared solutions provided ESI-MS analysis that confirmed the monomeric identity in solution. This apparent solution instability hampered attempts to obtain high-quality crystalline material, via slow evaporation of solvent, suitable for X-ray analysis. For example, solutions of **14a,b** in benzene-d_6 slowly decomposed over a 1-week period to unidentifiable material. Solid samples of **14a,b** were indefinitely stable at room temperature and in the absence of air; however, upon heating under reduced pressure at 175 °C, the pale-yellow solid turned black. Analysis of the resultant material by ^{1}H NMR revealed a mixture of unidentifiable products, but most noticeable was the loss of coordinated nitrile.

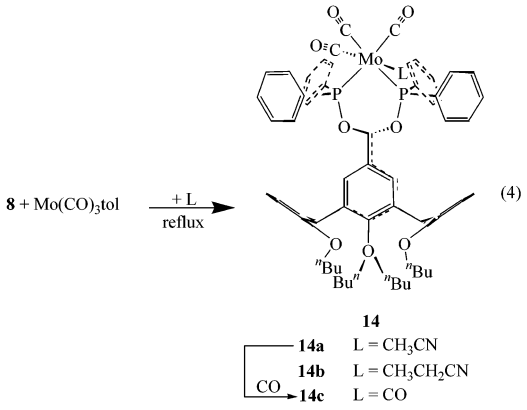

The ^{1}H NMR spectra of both complexes are quite similar and are reminiscent of that observed for **11**, in which the spatial orientation of the coordinated ligands gave rise to several inequivalent calix[4]arene hydrogen resonances,

Figure S3. For example, the bridging $ArCH_2Ar$ methylene resonances (AB spin system) appear as two sets of doublets, and the hydrogens ortho to the C(5) and C(17) carbon atoms appear as two doublets. Additional inequivalence is present in the arene region in which two sets of doublets and triplets are present for the hydrogens bound to the A and C rings. The most notable difference between that observed for **14a,b** and **12** is the presence of a well-defined AB quartet (4.47, 4.37; $^2J_{AB} = 12$ Hz). Another interesting aspect of the ^{1}H NMR spectra of **14a,b** to note is the upfield location of the methyl and ethyl hydrogen resonances of the appropriate nitrile ligands. In the case of **14a**, a singlet at 0.14 ppm was present, while for **14b** a triplet and quartet appeared −0.16 and 0.71 ppm, respectively. (This corresponds to shifts of about 2 ppm upfield from free ligand.) The initial expectation was that the ligand was directed toward the interior of the cavity, as examples exist in which metal−calix[4]arene chelates were capable of encapsulating a variety of small molecules.[4,7a,c] This scenario would require a meridonal orientation of the CO ligands and trans ligation of the tethered phosphinites. This formulation is inconsistent with the FT-IR data; moreover, this arrangement did not exist in the solid state as based on the acquisition of the somewhat poorly defined molecular structure of **14b**.

As mentioned above, acquisition of high-quality crystals for either **14a** or **14b** was not possible. Rapid recrystallization of both yielded platelike microcrystals. The crystal quality was poor, but **14b** yielded diffraction-quality crystals, wherein collection of a partial 2θ-data set provided an opportunity to elucidate the gross features of the inner- and outer-coordination sphere. The data, not shown, provide an informative ORTEP representation, which can be found in the Supporting Information (Figure S12). Like that observed in **12**, the bis(phosphinite) coordinates the molybdenum atom in a cis fashion, which is twisted above the pinched-cone, such that the original C_{2v} symmetry of the metal-free ligand is lost. The carbonyl ligands orient themselves facially in the Mo coordination sphere leaving the CH_3CH_2CN ligand bound to the Mo trans to a CO ligand. This picture shows that the C−H/π interactions that must be present, to account for the anomalous ^{1}H resonances, were due not to interaction with the inner annulus of the calix[4]arene cavity but with arene rings of the adjacent phosphinite ligand. The $CH_3-Ar_{centroid}$ distance observed in the solid state is 3.8 Å, which is about 0.1 Å beyond the sum of the van der Waals radii.[24] Inspection of the complex using a molecular modeling program showed that rotation of the propionitrile ligand about the C−N−Mo axis places the methyl group as close as 3.1 Å. This close contact readily explains the nature of the upfield ^{1}H NMR shift.

Complex **14a** readily underwent ligand substitution in the presence of gaseous CO and yielded the tetrakis(carbonyl) complex, **14c**, in 98% isolated yield, eq 4. This complex, unlike **14a,b**, is quite stable in solution, and solid samples were modestly air stable. The elemental analysis obtained for this compound agrees well with theory, and the FT-IR spectrum in the carbonyl region agrees with expectations. As with the aforementioned complexes, ESI-MS provided unambiguous evidence supporting the monomeric identity of **14c** in solution. The ^{1}H NMR spectrum of **14c**, in C_6D_6, closely resembles that of **12**. A singlet for the *meta*-hydrogens of rings B and D appeared at 6.38 ppm, and only two doublets were present for the $ArCH_2Ar$ axial and equatorial hydrogen atoms, while the methylene hydrogens, $ArCH_2OP-$, sampled magnetically equivalent environments, as deduced from the broadened singlet at 4.34 ppm. Inspection of the solid-state molecular structure of **14c** would seem to contradict the observed ^{1}H spectroscopic properties. Rationalization of these observables is possible if this system is capable of undergoing dynamic exchange.

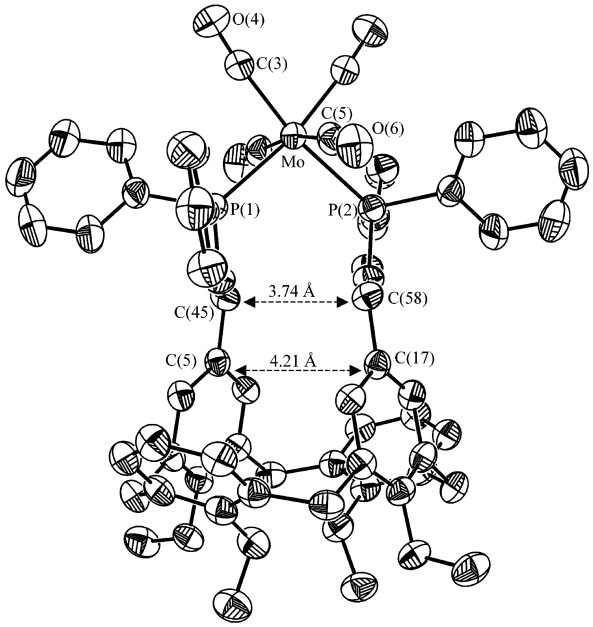

Figure 2. ORTEP representation (50% probability) of $Mo(CO)_4[(PPh_2OCH_2)_2$-^{n}Bu$_4$Clx], **14c** (including symmetry-equivalent atoms). Selected distances (Å) and bond angles (deg): Mo(1)−P(2) 2.4910(13), Mo(1)−C(3) 2.013(5), Mo(1)−C(5) 2.032(5), C(3)−O(4) 1.154(5), C(5)−O(6) 1.161(5), P(2)−Mo(1)−C(3) 170.43(12), P(2)−Mo(1)−C(5) 86.22(11), P(2)−Mo(1)−C(3)A 88.61(12), C(3)−Mo(1)−C(5) 91.23(17), C(3)−Mo(1)−C(3)A 82.6(2), C(5)−Mo(1)−C(5)A 168.5(2), C(5)···C(17) 4.21. Intraannular distances: C(5)···C(17), 4.21 Å; C(11)···C(23), 10.12 Å. Benzene solvate, alkyl chains, and hydrogens were omitted for clarity.

Figure 2 contains an ORTEP (50% probability) representation of the molecular structure of **14c**, in which the alkyl chains, hydrogens, and benzene solvate were omitted for clarity. Tables 1 and 2 provide selected crystallographic and metrical parameters for this complex. The material crystallized in the space group $P\bar{3}c1$, where the Mo atom resided in a special position. This presented a structure in which exactly half of the molecule was crystallographically unique. For the sake of uniformity, the depiction of **14c** shown in the figure contains the entire molecule and a numbering scheme consistent with the other structures reported herein. As observed in **12**, coordination of the metal fragment by the two opposing phosphinite moieties gave rise to a calix[4]arene structure best described as a "pinched-cone". This conformation resulted in an intraannular separation (C(5)···C(17)) of 4.21 Å and a C(45)···C(58) through-space

(24) Bondi, A. *J. Phys. Chem.* **1964**, *68*, 441−451.

distance of 3.74 Å. Due to crystallographically imposed symmetry, only one Mo−P bond is unique, and thus the carbonyls cis and trans are unique as well. As such, quoted distances and angles are not averages but the observed values. The two phosphorus atoms are ligated to the molybdenum (d(Mo−P2) = 2.488(1) Å) in a cis manner, but the nature of the calix[4]arene gives rise to an opened P−Mo−P angle of 100.42(5)°. This angle is much larger than other d^6-metal systems that contain the cis-chelated dppe ligand.[25] This is clearly a testament to the flexibility of the calix[4]arene macrocycle and is slightly larger than that observed in **12** (cf. 97.5°). The carbonyl trans to P2 gives normal Mo−C and C−O distances of 2.013(5) and 1.154(5) Å, respectively. As expected, the carbonyl cis to P2 gives an elongated Mo−C distance of 2.032(5) Å, but the C−O distance of 1.161(5) Å is statistically indistinguishable from its neighboring CO ligand. The coordination about the molybdenum is best described as pseudooctahedral, but the symmetry at the Mo is approximately C_{2v}. This is supported by the four CO stretches observed in the IR spectrum. While the symmetry of the metal approximates C_{2v} symmetry, the orientation in the figure shows that the entire molecule has approximate C_2 symmetry. This would suggest that the ^{1}H NMR spectrum is indeed a time-averaged spectrum (room temperature, 400.132 MHz), since the aforementioned resonances appear to be magnetically equivalent.

At the onset of this work, it was conceivable that a reduction in the linker from $-CH_2O-$ to $-CH_2-$ would provide a bidentate ligand that would readily chelate the metal center over an expanded cavity. Inspection of the molecular structure of **10**, Figure S10, shows that this ligand set should be ideally suited to accomplish such a feat. Unfortunately, the reaction of **10** with a stoichiometric amount of $Mo(CO)_3$(toluene), stirred in acetonitrile for 24 h with gentle heating, did not go to completion. Analysis of the isolated material by ^{1}H NMR showed the reaction to be incomplete; furthermore, neither longer reaction times (5 d) nor purification provided material free of starting material. It is believed that the material that formed was *fac*-$(CO)_3$Mo-$(NCCH_3)$[$(PPh_2CH_2)_2$-^{n}Bu$_4$Clx], **15**. ^{1}H NMR spectra proved difficult to interpret, but it was apparent that complexation occurred and most noticeable was the presence of an upfield singlet at −2.62 ppm. If the structure of **15** is similar to that observed for **14b,c**, then the anomalous shift would be attributable to a C−H/π interaction perhaps with the arene ring directly attached to P. ^{31}P NMR showed two doublets at 40.2 and 35.2 ppm (J = 27 Hz). This would require the molecular symmetry to be C_1, and unlike that observed for the other species reported herein, no operative dynamic exchange pathway. Inspection of the IR data showed four carbonyl stretches, which is consistent with cis-coordination by the **10**. In the course of manuscript revision, another article appeared in which the coordinative properties of 5,17-$(PPh_2CH_2)_2$-^{n}PrClx appeared.[9b] These authors failed to obtain chelated adducts with either (COD)PdMeCl or (COD)-$PtCl_2$ but, instead, isolated polymeric products. This observation was noted in an earlier study as well.[9a] In light of these two studies, it is possible that chelation did not occur, and the observed spectroscopic features of the isolated material were that of a polymeric adduct.

(25) (a) Kubas, G. J.; Burns, C. J.; Eckert, J.; Johnson, S. W.; Larson, A. C.; Vergamini, P. J.; Unkefer, C. J.; Khalsa, G. R. K.; Jackson, S. A.; Eisenstein, O. *J. Am. Chem. Soc.* **1993**, *115*, 569−581. (b) Luo, X. L.; Kubas, G. J.; Burns, C. J.; Eckert, J. *Inorg. Chem.* **1994**, *33*, 5219−5229. (c) King, W. A.; Luo, X. L.; Scott, B. L.; Kubas, G. J.; Zilm, K. W. *J. Am. Chem. Soc.* **1996**, *118*, 6782−6783.

Discussion

Solid-State Structures of Selected Tetra-O-alkylated Calix[4]arenes. The literature is rife with examples that suggest that the calix[4]arene cavities, when derivatized with reactive metal centers, are analogous to the active sites of metal-containing enzymes.[26] The hydrophobic pocket available within the confines of the calix[4]arene annulus, in practice, should provide additional stabilization for the preassociation of hydrophobic substrates prior to the occurrence of metal-mediated transformations. This aspect alone makes this class of host−guest molecules particularly attractive as applied in the area of homogeneous catalysis, as the presence of the cavity could provide added selectivity or varying reactivity. In light of this attribute, it seems important to highlight the observed solid-state parameters gleaned from this study and provide comparisons with other published calix[4]arene derivatives.

Table 3 contains data for tetra-O-alkylated calix[4]arenes (R_4Clx), with a few exceptions, showing the distances between opposing arenes (as measured by the through-space distances between C(5)···C(17) and C(11)···C(23)). The listed entries (E) fit nicely into three categories: (i) tetra-substitution at the upper rim (Y_4-R_4Clx, Y = H, E2−E4, Y = Br or NO_2, E5−E7); (ii) di-5,17-substitution at the upper rim (5,17-Y_2-11,23-H_2-R_4Clx (E9−E25, E29) or 5,17-Y_2-11,23-^{t}Bu$_4$-R_4Clx (E26−E28)); (iii) structurally determined metal chelates containing 5,17-calix[4]arene-containing ligands (E30−E42).

Given the data at hand, the first thing to recognize is the presence or absence of a cavity. The phenolic oxygens of the parent calix[4]arene cavities (**1** and **2**) participate in intramolecular hydrogen bonding, thereby enforcing the characteristic C_{4v}-symmetric cavity.[1] In the case of the parent calix-[4]arene, E1, the apparent symmetry is evident from the

(26) (a) Beer, P. D.; Drew, M. G. B.; Leeson, P. B.; Lyssenko, K.; Ogden, M. I. *J. Chem. Soc., Chem. Commun.* **1995**, 929−930. (b) Molenveld, P.; Kapsabelis, S.; Engbersen, J. F. J.; Reinhoudt, D. N. *J. Am. Chem. Soc.* **1997**, *119*, 2948−2949. (c) Blanchard, S.; Le Clainche, L.; Rager, M.-N.; Chansou, B.; Tuchagues, J.-P.; Duprat, A. F.; Le Mest, Y.; Reinaud, O. *Angew. Chem., Int. Ed.* **1998**, *37*, 2732−2735. (d) Molenveld, P.; Engbersen, J. F. J.; Kooijman, H.; Spek, A. L.; Reinhoudt, D. N. *J. Am. Chem. Soc.* **1998**, *120*, 6726−6737. (e) Xie, D.; Gutsche, C. D. *J. Org. Chem.* **1998**, *63*, 9270−9278. (f) Blanchard, S.; Rager, M.-N.; Duprat, A. F.; Reinaud, O. *New J. Chem.* **1998**, *22*, 1143−1146. (g) Molenveld, P.; Stikvoort, W. M. G.; Kooijman, H.; Spek, A. L.; Engbersen, J. F. J.; Reinhoudt, D. N. *J. Org. Chem.* **1999**, *64*, 3896−3906. (h) Molendveld, P.; Engbersen, J. F. J.; Reinhoudt, D. N. *J. Org. Chem.* **1999**, *64*, 6337−6341. (i) Rondelez, Y.; Seneque, O.; Rager, M.-N.; Duprat, A. F.; Reinaud, O. *Chem.—Eur. J.* **2000**, *6*, 4218−4226. (j) Clainche, L. L.; Giorgi, M.; Reinaud, O. *Eur. J. Inorg. Chem.* **2000**, 1931−1933. (k) Clainche, L. L.; Giorgi, M.; Reinaud, O. *Inorg. Chem.* **2000**, *39*, 3436−3437. (l) Rondelez, Y.; Rager, M.-N.; Duprat, A.; Reinaud, O. *J. Am. Chem. Soc.* **2002**, *124*, 1334−1340. (m) Spencer, D. J. E.; Johnson, B. J.; Johnson, B. J.; Tolman, W. B. *Org. Lett.* **2002**, *4*, 1391−1393.

Table 3. Pinched-Cone Arene-to-Arene Distances for Selected Calix[4]arenes

entry	compd	C(5)···C(17) (Å)	C(11)···C(23) (Å)	ref
1	Clx[a]	8.39	8.39	27a
2	^{n}Bu$_4$Clx, **3**	4.22	10.06	this work
3	(CH$_3$SCH$_2$CH$_2$)$_4$Clx	4.97	9.64	28
4	(CH$_2$CH$_2$OH)$_4$Clx	4.54	9.79	29
5	Br$_4$-^{n}Bu$_4$Clx, **4**[b]	4.45(13)	10.02(8)	this work
6	Br$_4$-^{n}Pr$_4$Clx·C$_{60}$[c]	5.08	9.96	30
7	(NO$_2$)$_4$-^{n}Pr$_4$Clx	4.64	9.97	31
8	(NO$_2$)$_2$-^{n}Pr$_4$Clx	4.04	10.11	32
9	^{t}Bu$_2$-R$_4$Clx[d]	10.061	4.958	33
10	Ph$_2$-^{n}Pr$_4$Clx	10.11	4.35	34
11	Y$_2$-^{n}Pr$_4$-Clx[e]	9.97	4.61	35
12	Y$_2$-^{n}Pr$_4$-Clx[f]	9.96	4.41	35
13	(3-Br-Ph)$_2$-^{n}Pr$_4$Clx	10.10	4.11	34
14	1-Nap$_2$-^{n}Pr$_4$Clx[g]	4.96	9.64	34
15	Carb$_2$-^{n}Pr$_4$Clx[h]	4.95	9.52	34
16	Y$_2$-^{n}Pr$_4$Clx[i]	5.36	9.48	19
17	Br$_2$-^{n}Bu$_4$Clx, **5**	4.37	9.92	this work
18	Br$_2$-Bz$_4$Clx[b]	9.8(1)	4.50(8)	7b
19	(CHO)$_2$-^{n}Bu$_4$Clx, **6**	3.90	10.12	this work
20	(HOCH$_2$)$_2$-^{n}Bu$_4$Clx, **7** (**A**)[j]	9.71	4.94	this work
21	(HOCH$_2$)$_2$-^{n}Bu$_4$Clx, **7** (**B**)[j]	4.41	9.88	this work
22	(HOCH$_2$)$_2$-^{n}Bu$_4$Clx, **7** (**C**)[j]	10.09	3.78	this work
23	(PPh$_2$OCH$_2$)$_2$-^{n}Bu$_4$Clx, **8**	10.02	4.20	this work
24	(PPh$_2$CH$_2$)$_2$-^{n}Bu$_4$Clx, **10**	4.51	10.11	this work
25	(PPh$_2$CH$_2$)$_2$-^{n}Pr$_4$Clx	4.54	10.13	9b
26	^{t}Bu$_4$-^{n}Pr$_4$Clx	7.83	7.79	32
27	5,17-(P(O)Ph$_2$CH$_2$)$_2$-11,23-^{t}Bu$_2$-^{n}Pr$_4$Clx[k]	6.45	9.21	9a
28	5,17-^{t}Bu$_2$-11,23-cht$_2$-R$_4$Clx[d,l]	5.91	9.32	33
29	S$_2$Clx[m]	6.43	9.19	4b
30	Cl$_2$Ru(CO)$_2$[5,17-(PPh$_2$)$_2$-^{n}Pr$_4$Clx][n]	5.62	9.63	7a
31	[Ag-^{n}Pr$_4$Clx]OTf[o]	4.78	9.89	36b
32	{*trans*-Cl$_2$Pd[(PPh$_2$)$_2$-Bz$_4$Clx]}$_2$[p]	10.18	4.06	7b
33	*cis*-Cl$_2$Pt[(PPh$_2$)$_2$-Bz$_4$Clx][q]	4.19	9.96	7b
34	5,17-(Cp′$_2$)Co-*O*-5,*O*-17-Tos$_2$Clx^{+}[r]	4.24	10.36	5
35	5,17-(Cp′CoCp)$_2$-*O*-5,*O*-17-Tos$_2$Clx^{2+}[s]	7.15	8.97	5
36	5,17-(Cp′FeCp)$_2$-*O*-5,*O*-17-Tos$_2$Clx[s]	9.49	6.20	5
37	Cp*Cl$_2$Rh(5-(PPh$_2$)-^{n}Pr$_4$Clx][t]	4.92	9.60	8b
38	(η^3-C$_4$H$_7$)Pd[(PPh$_2$)$_2$-^{n}Pr$_4$Clx]	4.19	10.17	7c
39	*cis*-Cl$_2$Pt[(PPh$_2$)$_2$-^{n}Pr$_4$Clx′][q,u]	10.17	4.18	7c
40	*cis*-Cl$_2$(*p*-cymene)Ru[(PPh$_2$)-^{n}Pr$_4$Clx′][v]	6.21	9.21	7c
41	*cis*-Cl$_2$Pd[(PPh$_2$OCH$_2$)$_2$-^{n}Bu$_4$Clx], **12**	4.27	10.14	this work
42	Mo(CO)$_4$[(PPh$_2$OCH$_2$)$_2$-^{n}Bu$_4$Clx], **14c**	4.21	10.12	this work

[a] Acetone solvate outside of cavity. [b] Average value of two crystallographically unique molecules in the unit cell. [c] C$_{60}$ as cocrystallate. [d] R = *tert*-butyloxycarbonyl. [e] Y = 2-(2-bromophenyl)ethenyl. [f] Y = 2-(4-bromophenyl)ethenyl. [g] 1-Naphthalyl. [h] *N*-Carbazolyl. [i] Y = fluorenyl. [j] Cystallographically unique molecules in the unit cell. [k] R = EtOEt. [l] cht = cyclohepta-2,4,6-trienyl. [m] 5,17-(α,α′-*m*-Xylenedithioacetamide)-tetra-25,26,27,28-*n*-propoxycalix[4]arene (S$_2$Clx). [n] Phosphines, chlorides, and carbonyls are all trans, with the CO inside the pocket. [o] Ag(I) positioned at midpoint between line joining C(5) and C(17). [p] Dimeric species. [q] Molecular structure showed Cl$_2$Pt fragment over half of the annulus. [r] 5,17-Positions possess formamidocyclopentadienyl substituents, NHC(O)C$_5$H$_4$, which when in pinched-cone conformation create a cobaltacenium complex. [s] Cp′ = (C$_5$H$_4$)C(O)NH−. [t] Cp*RhCl$_2$ fragment directed away from the pinched-cone in the solid state. [u] Clx′ = 5,17-Br$_2$-11,23-(PPh$_2$)$_2$-^{n}Pr$_4$Clx. [v] Clx′ = 5,11,17-Br$_3$-23-PPh$_2$-^{n}Pr$_4$Clx.

equivalent distances of 8.39 Å.[27] These molecular dimensions afford a cavity with an estimated van der Waals volume (V_{vdW}) of approximately 36−52 Å^3.[24] This cavity enforcing interaction is lost upon tetra-O-alkylation, where the calix[4]arene cavity adopts a C_{2v}-symmetric, or "pinched-cone", conformation. This is evident upon inspection of the values in E2−E25, where the average pinched-arene distance is 4.5 ± 0.4 Å[7b,19,28−35] and the estimated V_{vdW} is 8−20 Å^3. It is interesting to note that the sole purpose of tetra-O-alkylation is to suppress the formation of intraannular conformations, such as the partial-cone, 1,2- and 1,3-alternate structures, and thereby retain the conelike shape of the calix[4]arene.[1] Yet, it is obvious from the data that this modification clearly reduces the effective volume of the cavity to a point where it seems inaccurate to refer to these species as "bowl-shaped"

(27) (a) Ungaro, R.; Pochini, A.; Andreetti, G. D.; Sangermano, V. *J. Chem. Soc, Perkin Trans 2* **1984**, 1979−1985. (b) Harrowfield, J. M.; Ogden, M. I.; Richmond, W. R.; Skelton, B. W.; White, A. H. *J. Chem. Soc., Perkin Trans. 2* **1993**, 2183-2190. (c) Akdas, H.; Bringel, L.; Graf, E.; Hosseini, M. W.; Mislin, G.; Pansanel, J.; De Cian, A.; Fisher, J. *Tetrahedron Lett.* **1998**, *39*, 2311−2314.

(28) Yordanov, A. T.; Whittlesey, B. R.; Roundhill, D. M. *Inorg. Chem.* **1998**, *37*, 3526−3531.

(29) Moran, J. K.; Georgiev, E. M.; Yordanov, A. T.; Magu, J. T.; Roundhill, D. M. *J. Org. Chem.* **1994**, *59*, 5990−5998.

(30) Barbour, L. J.; Orr, G. W.; Atwood, J. L. *Chem. Commun.* **1998**, 1901−1902.

(31) Kenis, P. J. A.; Noordman, O. F. J.; Houbrechts, S.; van Hummel, G. J.; Harkema, S.; van Veggel, F. C. J. M.; Clays, K.; Engbersen, J. F. J.; Persoons, A.; van Hulst, N. F.; Reinhoudt, D. N. *J. Am. Chem. Soc.* **1998**, *120*, 7875−7883.

(32) Verboom, W.; Struck, O.; Reinhoudt, D. N.; van Duynhoven, J. P. M.; van Hummel, G. J.; Harkema, S.; Udachin, K. A.; Ripmeester, J. A. *Gazz. Chim. Ital.* **1997**, *127*, 727−739.

(33) Orda-Zgadzaj, M.; Wendel, V.; Fehlinger, M.; Ziemer, B.; Abraham, W. *Eur. J. Org. Chem.* **2001**, 1549.

(34) Larsen, M.; Krebs, F. C.; Harrit, N.; Jorgensen, M. *J. Chem. Soc., Perkin Trans. 2* **1999**, 1749−1757.

(35) Larsen, M.; Krebs, F. C.; Jorgensen, M.; Harrit, N. *J. Org. Chem.* **1998**, *63*, 4420−4424.

derivatives, as the name implies the ability to contain.[36] In the absence of any other factors, see below, the calix[4]arene species listed here that possess the "pinched-cone" conformation but still may be called cavity-containing molecules are found in E26−E29.[4b,9,32,33] The increased arene-to-arene separation for the first three must be due to the C(11) and C(23) *tert*-butyl substituents, while the last one is brought about by a spanning functionality that fixes the intraannular separation.

Since it is well-known that R_4Clx species undergo a rapid exchange between two C_{2v}-symmetric species,[36] i.e., one conformer in which the C(5)···C(17) separation is short and another in which this distance is large, then it comes to no surprise that these molecules crystallize in two conformational forms. For the sake of discussion, an "open" conformation is one in which a C_{2v}-symmetric calix[4]arene species possesses a large C(5)···C(17) distance and a "closed" conformation will be used to denote a short arene-to-arene separation. Given the limited data, E8, E17, and E19, it would appear that when Y is small, the "closed" conformation is preferred (E18 is an exception), and the converse is true when Y is large, E9−E13 and E23. Disruption of this trend occurs when the two substituents are capable of interacting with one another. For example, complexes that possess the closed conformation (E12−E16, E23, and E25) presumably adopt this configuration due to the presence of either $\pi-\pi$ interactions (E14 and E15) or C−H/π interactions (E16, E24, and E25) or some unforeseen crystal packing forces. In addition, for the hydroxymethyl species (**7**, E20−E22), intramolecular hydrogen bonding (O···O separation of 2.75(3) Å) promoted the "closed" conformation, but intermolecular hydrogen bonding (with lattice solvent) gave rise to the "open" conformation. These data clearly show that the preferred solid-state conformation for unconstrained tetra-O-alkylated calix[4]arenes is a pinched-cone. As such, metal complexes should exhibit similar solid-state properties in which the volume of the calix[4]arene cavity is significantly diminished relative to the parent calix[4]arenes, E1.

Solid-State Structures of Selected Tetra-O-alkylated Metal−Calix[4]arene Complexes. As mentioned in the introductory remarks, the long-term goal is to situate reactive metal fragments above the opened mouth of the calix[4]arene such that the hydrophobic pocket can be used to promote association of alkanes in close proximity to a reactive metal center. To date, several examples exist in which positioning of the metal above the binding-cleft occurred,[4,7−9] and only one of these investigators indicated that hydrocarbon activation is the thrust of future research.[8] For example, Loeb et al. were the first to prove that the cavity is large enough to accommodate small ligands when a metal resides above the mouth of the cavity.[4] They employed the ligand, E29, which is capable of undergoing cyclometalation with Pd(II) to form a cationic R′(SCS)Pd−^{n}Pr$_4$Clx adduct. This study did not produce a molecular structure of the resultant complexes, but ^{1}H NMR data confirmed the encapsulation of small ligands, CH_3CN and pyr, above the mouth of the cavity.

Matt et al., E30, reported a remarkable example of the inclusion of a small ligand, CO, within the reduced confines of the calix[4]arene.[7a] In this calix[4]arene complex, the Ru(II) adopted an all-trans coordination sphere in which 5,-17-bis(phosphines) provided a metal complex in which entrapment of the coordinated carbonyl occurred. Given the C(5)···C(17) distance of 5.62 Å, this should be considered a remarkable feat, as the CO-to-arene distance is 2.70 Å and is well within the van der Waals radii of the observed atoms.[24] A third example in which metal complexation above the mouth of the cavity occurred appears in E31.[36b] This complex showed that the *para*-carbons of rings B and D interact with Ag(I) in an η^1-fashion. This mode of coordination is now known to be somewhat common,[37] but the two-coordinate silver coordination sphere, with a C(5)···Ag(I)···C(17) angle of 173°, makes this entity unique.

Tsuji et al. recently prepared Pd(II)− and Pt(II)−calix-[4]arene analogues, E32 and E33, in which the same ligand coordinated the metals in two strikingly different ways.[7b] In the case of the complexes listed in E32 and E33, trans ligation of the bis(phosphine) ligand to Pd(II) occurred for the former, but cis-ligation to Pt(II) in the latter. Given the fact that these disubstituted calix[4]arenes undergo the aforementioned $C_{2v}-C_{2v}$ interconversion,[36] it becomes clear why this ligand is capable of either chelation (E33) or dimerization (E32). It would appear that the synthetic conditions, and the nature of the metal, dictate the outcome of coordination. Both complexes revealed a normal C(5)···C(17) distance, and the $PtCl_2$ fragment resided on one side of the cavity. The occupation of the Pt(II) coordination array over a hydrophobic cleft would suggest that this species, when appropriately derivatized, should be ideally suited to participate in selective C−H activation. The complexes prepared by Beer et al. are different from all other entries, in that only two of the four phenolic oxygens were functionalized, E35 and E36.[5] Coupled with the presence of bulky sandwich complexes, this arrangement afforded calix-[4]arene derivatives with well-defined cavities as evidenced by the larger than normal C(5)···C(17) distances of about 8.1 Å. Indeed, these authors found that these molecules served as anion receptors in which a change in potentials of the electrochemically active species provided an opportunity to sense different anions.

Harvey et al. prepared 5-PR_2-^{n}Pr$_4$Clx (R = Ph, ^{i}Pr) derivatives capable of coordinating Rh(III) (E37).[8] This was a clever design in which a potential Rh(I) species might undergo selective C−H activation with alkanes that could undergo preassociation due to the positioning of the rhodium

(36) (a) Conner, M.; Janout, V.; Regen, S. L. *J. Am. Chem. Soc.* **1991**, *113*, 9670−9671. (b) Ikeda, A.; Tsuzuki, H.; Shinkai, S. *J. Chem. Soc., Perkin Trans. 2* **1994**, 2073−2080.

(37) (a) Shelly, K.; Finster, D. C.; Lee, Y. J.; Scheidt, W. R.; Reed, C. A. *J. Am. Chem. Soc.* **1985**, *107*, 5955−5959. (b) Xie, Z.; Wu, B.-M.; Mak, T. C. W.; Manning, J.; Reed, C. A. *J. Chem. Soc., Dalton Trans.* **1997**, 1213−1217. (c) Munakata, M.; Wu, L. P.; Kuroda-Sowa, T.; Maekawa, M.; Suenaga, Y.; Sugimoto, K.; Ino, I. *J. Chem. Soc., Dalton Trans.* **1999**, 373−378. (d) Batsanov, A. S.; Crabtree, S. P.; Howard, J. A. K.; Lehmann, C. W.; Kilner, M. *J. Organomet. Chem.* **1998**, *550*, 59−61. (e) Tsang, C.-W.; Yang, Q.; Sze, E. T.-P.; Mak, T. C. W.; Chan, D. T. W.; Xie, Z. *Inorg. Chem.* **2000**, *39*, 5851−5858.

fragment relative to the cavity. Inspection of the solid-state structure showed that the reactive part of the rhodium coordination sphere would appear to be directed away from the mouth of the cavity. These authors discovered that a dynamic exchange pathway could give rise to a conformer which would position the more reactive part of the fragment above the annulus, but inspection of the C(5)···C(17) distance (ca. 5 Å) shows that, rather than a cavity, a partial cleft would be available to interact with alkanes prior to reaction with the rhodium center.

Finally, a recent report by Matt et al. revealed that complexation of Pd, Pt, and Ru occurred using either di- or monosubstituted calix[4]arenes, E38−E40.[7c] Both Pd and Pt adducts closely resemble Tsuji's complex, with close C(5)···C(17) contacts and the positioning of the metal fragment over half of the pinched-cone. The Ru adduct, E40, is remarkable in that the *p*-cymene ligand seemed to be "encapsulated" within the enlarged annulus of the cavity (cf. C(11)···C(23) distance of 6.21 Å). This structure bears a striking similarity to a calculated structure obtained for $Cp^*Cl_2Rh[5\text{-}(PPh_2)\text{-}{}^nPr_4Clx]$.[8b] In the case of the complex shown in E40, ^1H NMR revealed that the encapsulation of the *p*-cymene moiety was persistent in solution.

Given the complexes listed above, the structures reported herein, and some selected literature examples (see below), it is now clear that there are several ways of accomplishing metal coordination over a calix[4]arene cavity. The factors that dictate the mode of coordination, i.e., cis or trans, or the formation of monomers, dimers, or polymeric species are slowly becoming apparent. At present, only one report exists in which a functionally modified calix[4]arene resulted in metal chelation above an opened calix[4]arene hydrophobic pocket.[4] All other variations seem to be complicated by the conformational flexibility of these systems, such that the metal actually resides over a hydrophobic cleft.[7−9] It should be clear that additional studies are necessary in order to determine the precise ligand properties that will present a metal-fragment above a well-defined cavity. This property is crucial to the realization of our long-term goal of discovering more examples of alkane−metal complexes. Of all the published examples, Loeb's ligand seems to be an attractive candidate for such studies. This is especially true when one considers the ability of $R(PCP)Ir^I$ adducts to undergo alkane activation.[38] Conceivably, an Ir(I) adduct, using this ligand, would provide the ideal system to affect such transformations. The reactive part of the molecule would be directed toward the interior of the cavity and, given the size constraints, may serve to inhibit the process of olefin isomerization which is known to occur in R(PCP)Ir catalytic systems. Functionalization of the calix[4]arene with longer alkyl chains, e.g., C6−C10, would increase the solubility in alkane only solvent systems. Except for the two provided reports,[4] it is unclear if this investigator is interested in pursuing this line of research.

Other attractive candidates occur in the examples provided by Matt and Tsuji in which the $PtCl_2$ fragment resides over half of the cavity. While the binding pocket should really only be classified as a binding-cleft, the availability of the splayed arene could promote selectivity in alkane functionalization. A deeper, more voluminous, binding pocket is synthetically accessible upon the introduction of benzyl substituents at the C(11) and C(23) positions.[39] Harvey's system seems promising if, and only if, the reactive fragment was found not only above the hydrophobic cleft but directed toward it. The authors stated that the Rh(I) complex undergoes C−H activation, and it will be interesting to see if any selectivity occurs in this system. Inspection of the molecular structures of **12** and **14c** reveals that diametrically functionalized species prepared herein render a metal coordination sphere in which any subsequent reactivity would occur directed away from the hydrophobic cleft. Even if a rollover motion occurred, see below, the metal would be well removed from the hydrophobic confines of the calix[4]arene.

One possibility that, to our knowledge, has not been tested is to metalate the lower rim phenoxide atoms, thereby enforcing an enlarged cavity, but then introduce traditional P-ligands at the upper-rim positions. For example, Floriani, and others, reported $[M]O_4Clx$ species that provide cavities with an intraannular volume that approaches that of the C_{4v}-symmetric parent molecule. These complexes, $(O)WO_4Clx(O{=}C(CCH_3)_2)$,[40] $(cat')WO_4Clx$,[41] Cp^*TaO_4Clx,[42] and $(ArN)MoO_4Clx(NCCH_3)$,[43] provide C(5)···C(17) distances that range from 7.3 to 8.3 Å. This enlarged cavity would then require longer linkers that tether the ligand to the cavity, e.g., either $-CH_2CH_2-$ or $-CH_2O-$, to promote chelation above the mouth of the calix[4]arene. This seems to be feasible but would be synthetically challenging, as it is uncertain that the metals used to enforce the cavity would survive the many steps required to achieve functionalization along the upper rim. An alternative route would be to introduce upper-rim substituents using the tetra-O-benzoylated derivatives,[1] where removal of the benzoyl groups followed by formation of aryloxy−metal chelates would afford a bidentate ligand with a well-defined cavity.

Conformational Exchange Available to Metal−Calix[4]arene Chelates. The data reported herein would not be complete without considering the possible dynamic exchange that is available to these systems. The molecular structures of $cis\text{-}Cl_2Pt[(PPh_2)_2\text{-}R_4Clx]$[7b,c] and $(\eta^3\text{-}C_4H_7)Pd[(PPh_2)_2\text{-}{}^nPr_4\text{-}Clx]$[7c] showed that the metal fragment resided over half of the calix[4]arene, e.g., the A or C ring, though NMR data suggested the presence of reflective elements present in the molecule. Both authors independently proposed a dynamic exchange pathway that rationalizes the observed NMR data

(38) (a) Liu, F.; Pak, E. B.; Singh, B.; Jensen, C. M.; Goldman, A. S. *J. Am. Chem. Soc.* **1999**, *121*, 4086−4087. (b) Liu, F.; Goldman, A. S. *Chem. Commun.* **1999**, 655−656.

(39) Arduini, A.; Pochini, A.; Rizzi, A.; Sicuri, A. R.; Ugozzoli, F.; Ungaro, R. *Tetrahedron* **1992**, *48*, 905−912.

(40) Corazza, F.; Floriani, Chiesi-Villa, A.; Rizzoli, C. *Inorg. Chem.* **1991**, *30*, 4465−4468.

(41) Vigalok, A.; Zhu, Z.; Swager, T. M. *J. Am. Chem. Soc.* **2001**, *123*, 7917−7918.

(42) Acho, J. A.; Doerrer, L. H.; Lippard, S. J. *Inorg. Chem.* **1995**, *34*, 2542−2556.

(43) Gibson, V. C.; Redshaw, C.; Clegg, W.; Elsegood *J. Chem. Soc., Chem. Commun.* **1995**, 2371−2372.

Scheme 2

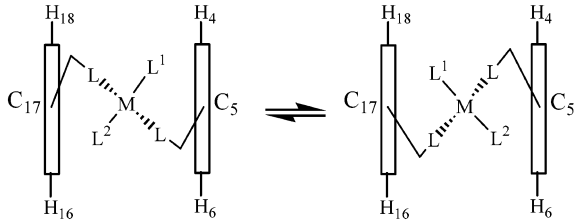

by schematically showing that the metal may reside on either side of the calix[4]arene by undergoing what Tsuji called a "rollover motion".[7b] An additional motion described by Tsuji was called a "twist-motion". This latter motion does not result in the "flipping" of the $PtCl_2$ fragment from half of the calix[4]arene to the other but appeared to be a process that resulted in a contortion of the inner coordination sphere as a result of partial rotation about the C−P bond.

It seemed possible that some mode of exchange must occur for the complexes prepared herein to account for the observed room-temperature ^{1}H NMR spectra. The diagnostic hydrogens to note are the methylene hydrogens (**I**, $ArCH_2Ar$) and the *meta*-arene hydrogens (**II**, H4, H6, H16, and H18) of rings B and D. Scheme 2 shows a partial representation of two metal−calix[4]arene adducts (where the B and D rings appear as rectangles with the carbons bearing the ligand substituents labeled as C_5 and C_{17}) that undergo exchange with one another by a simple rotation about the $-CH_2-$C(5/17) bonds. The complexes prepared in this study have the following identities, using the formalism in Scheme 2: **11**, M = Ti, L = $-CH_2O-$, $L^1 = CH_3$, L^2 = Cp; **12**, M = Pd, L = $-CH_2OPPh_2$, $L^1 = L^2$ = nothing, Cls omitted for clarity; **14a,b**, M = Mo, L = $-CH_2OPPh_2$, L^1 = CO L^2 = NCR, COs omitted for clarity; **14c**, L = $-CH_2OPPh_2$, $L^1 = L^2$ = CO). The ^{1}H NMR spectra of **11** and **14a,b** gave rise to similar patterns for the diagnostic hydrogens, while **12** and **14c** yield common spectral characteristics. In the absence of dynamic exchange, the C_1-symmetric complexes, **11** and **14a,b**, should yield four doublets each for the diagnostic hydrogens of types **I** and **II**, while the C_2-symmetric complexes, **12** and **14c**, should yield two doublets each for the reporter hydrogens (**I** and **II**). Since this was not observed, then the twisting motion shown in Scheme 2 served to raise the average symmetry observed in solution to C_s, for **11** and **14a,b**, and to C_{2v}, for **12** and **14c**. Low-temperature (−80 °C) ^{1}H NMR for these complexes revealed only slight broadening of the diagnostic hydrogen resonances. This suggests that this exchange pathway is very rapid on the NMR time scale (400.132 MHz). In light of the rate with which this process occurs, it now seems prudent to suggest that the inequivalence observed by Matt et al. for (η^3-C_4H_7)Pd[5,17-$(P(OEt)_2OCH_2)_2$-11,23-^{t}Bu-EtOEt$_4$Clx$^+$ must surely be due to the orientation of the η^3-C_4H_7 ligand.[9a] This supposition is bolstered by Tsuji's data showing two distinct orientations for an η^3-C_3H_5 ligand in (η^3-C_3H_5)Pd[$(PPh_2)_2$-Bz$_4$Clx]BF_4.[7b]

Conclusions

This study presents the preparation of three new calix[4]-arene ligands using a variety of literature protocols. The large-scale preparation of the parent *tert*-butylcalix[4]arene from 4-*tert*-butylphenol provided ample quantities of starting material for the extended synthetic sequence used herein. The choice of *n*-butyl lower-rim substituents provided intermediates, ligands, and metal complexes that were, save a few exceptions, readily crystalline and amenable to X-ray crystallographic analysis. A comparison of the structures reported herein, with previously published 5,17-diametrically substituted calix[4]arenes, confirmed the configuration as a pinched-cone.

The two ligands, **7** and **8**, chelated Ti, Pd, and Mo depending upon the nature of the ligand. Though not discussed, chelates of Pt and W were realized, using ligand **8** and conditions similar to that described for Pd and Mo, respectively. All bidentate ligands coordinate the metal in a cis-fashion. An alkoxy-based calix[4]arene, **7**, effectively chelated the CpTi(Me) fragment. The isolated material was not readily crystalline, but the ^{1}H NMR data showed that the structure was consistent with chelation above the pinched-cone in a twisted manner.

A bis(diphenylphosphinito)calix[4]arene ligand, **8**, afforded chelates with Mo, W, Pd, and Pt using the appropriate starting materials. The palladium adduct was thoroughly characterized using a battery of techniques and was found to be monomeric in which chelation occurred above the pinched-cone. The solid-state structure confirmed the coordination mode and coupled with the ^{1}H NMR data revealed the presence of a dynamic exchange pathway. This complex was found to be susceptible to acid-promoted decomposition, in which the products were [μ_2-ClPd(PPh_2OH)(PPh_2O)]$_2$ and **9**.

As with the palladium complex, the molybdenum, for **14a**−**c**, was situated above the "closed-mouth" of the calix-[4]arene cavity. ^{1}H NMR of **14a,b** revealed that C−H/π interactions existed between the coordinated nitriles and some part of the complex in solution, where the respective proton resonances were shifted upfield by about 2 ppm, relative to free nitrile. A partial solution of the molecular structure of **14b** showed that the origin of this anomalous chemical shift was due to an interaction that existed between the ligated nitrile and a phenyl ring of the coordinated phosphinite. This result should serve as a fair warning, however, as when there are two types of arene rings present in the calix[4]arene derivative, observation of uncharacteristic ^{1}H NMR shifts cannot be readily attributed to interactions with the inner walls of the cavity. An X-ray crystallographic study of the Mo(CO)$_4$-^{n}Bu$_4$Clx, **14c**, revealed that coordination to the metal by the bidentate ligand occurs in a cis-fashion, where the IR data supported the local C_{2v} symmetry about the molybdenum atom.

Preparation of the bis(diphenylphosphino)calix[4]arene ligand, **10**, occurred using known procedures, and its coordinative properties were examined. Reaction with Mo(CO)$_3$-(toluene) in acetonitrile showed that coordination occurred, but the reaction was incomplete. In light of Kubas' work, and the absence of a solid-state structure, it is impossible to state conclusively whether chelated or polymeric adducts formed under these reaction conditions.

A survey of the solid-state structures reported herein

showed that the pinched-cone conformation adopted by calix[4]arenes reduces the effective cavity volume to the point that care should be taken when designating the molecules as either "bowl-shaped" or "cavity-containing". Inspection of these structures showed that the 5,17-substituents prefer a "closed" conformation when small or when there are stabilizing factors present but adopt an "open" conformation when sufficiently bulky. A brief review of the currently available literature showed that the "closed" conformation is present in cis-chelated metal complexes but that the trans complexes gave rise to an expanded cavity. The only way presently known to situate metals above a voluminous cavity is to tether a rigid linker that constrains the calix[4]arene in an opened conformation. The metal complexes reported herein showed that there is binding of the metal fragment above the pinched-cone, but the metal is too far removed from the binding cleft to even suggest that the any participation in selective catalysis would occur. This is not true for several other reported complexes, and it will be interesting to see if any selectivity is possible for these systems.

Finally, the rationalization of the observed ^{1}H NMR spectroscopic features reported herein is possible when one considers a simple twisting motion of the coordination sphere above the pinched-cone of the calix[4]arene annulus. This motion occurred by rotation about the $-CH_2-C(5/17)$ bonds which raised the average symmetry of the complexes in solution. Future work will continue with the aim of achieving an organometallic species capable of binding alkanes that reside within the interior of the cavity.

Experimental Section

Unless otherwise noted, all reactions were carried out under an atmosphere of helium, argon, or nitrogen. Solvents were appropriately dried and degassed prior to use. $ClPPh_2$ (95%) was purchased from Aldrich and used without further purification. Carbon monoxide was purchased from Scott Specialty Gases, Inc. $Mo(CO)_3$(toluene)[44] and *cis*-$Cl_2Pd(PhCN)_2$[45] were prepared as directed in the literature. IR spectra were obtained from a Nicolet 5DXC FTIR spectrophotometer. ^{1}H, ^{13}C, and ^{31}P NMR spectra were collected at operating frequencies of 400.132, 100.625, and 161.975 MHz, respectively, using a Bruker DRX-400 spectrometer. ^{1}H and ^{13}C NMR were referenced relative to internal TMS or solvent, and ^{31}P NMR data were referenced to external H_3PO_4. Fast atom bombardment (FAB) mass spectrometry was performed on a VG7070E magnetic sector mass spectrometer. Midwest Microlab, LLC (Indianapolis, IN), provided elemental analysis for the calix[4]arene derivatives (**2**−**10**), while all other species were analyzed using Desert Analytics (Tucson, AZ). All solids were heated in a vacuum oven at a temperature that ensured complete removal of lattice solvents. Electrospray mass spectrometry was operated in the positive-ion mode using a Micromass QTOF II (Beverly, MA). Samples, in the appropriate solvent, were directly infused using a syringe pump operating at 5 μL/min. High-resolution spectra were recorded with poly-D-alanine as an internal molecular weight standard. X-ray analyses were performed using a Bruker SMART CCD system operating at −80 °C (vide infra). Synthetic procedures and spectroscopic data for **1**−**6** and **9** are available in the Experimental Section of the Supporting Information. All X-ray crystallographic details are available in the Supporting Information.

5,17-Dihydroxo-25,26,27,28-tetra-*n*-butoxycalix[4]arene, $(HOCH_2)_2$-^{n}Bu$_4$Clx, 7.[9a] The preparation of this material was achieved using a previously published procedure.[9a] X-ray-quality crystals were obtained in a freezer upon slow evaporation of a solution of **7** in diethyl ether/methanol. Great care was required to mount the crystals as lattice solvent was immediately lost upon removal from the mother liquor. ^{1}H NMR (δ, ppm; C_6D_6): 7.00 (d, 4H, ArH), 6.87 (t, 2H, ArH), 6.60 (s, 4H, ArH), 4.58 (d, $^2J_{HH}$ = 13.2 Hz, 4H, $ArCH_2Ar$), 4.19 (s, 4H, $ArCH_2OH$), 4.08 and 3.77 (t, $^3J_{HH}$ = 7.1 Hz, 8H, $ArOCH_2$), 3.19 (d, $^2J_{HH}$ = 13.2 Hz, 4H, $ArCH_2Ar$), 2.27 (br s, 2H, OH), 2.00 and 1.85 (quint, $^3J_{HH}$ = 7.1 Hz, 8H, OCH_2CH_2Et), 1.47 and 1.34 (hex, $^3J_{HH}$ = 7.1 Hz, 8H, $O(CH_2)_2CH_2Me$), 0.99 and 0.98 (t, $^3J_{HH}$ = 7.1 Hz, 12H, CH_3). ^{13}C NMR (δ, ppm; $CDCl_3$): 157.13, 155.49, 136.00, 134.32, 134.10, 128.68, 126.36, 122.13, 75.10, 74.83, 64.72, 32.47, 32.07, 31.01, 19.54, 19.18, 14.18, and 14.04. MS (FAB; *m*/*z*): MH^+ = 709.4. Anal. Found for crystalline material: C, 76.27; H, 7.64. Calcd for $C_{46}H_{60}O_6$ (M_r = 708.97): C, 77.93; H, 8.53. The results were consistent with the presence of CH_3OH in the lattice. Extended heating under vacuo (110 °C, 48 h, 5 mTorr) resulted in a loss of crystallinity but gave excellent agreement with theory.

5,17-Bis((diphenylphosphinito)methyl)-25,26,27,28-tetra-*n*-butoxycalix[4]arene, $(PPh_2OCH_2)_2$-^{n}Bu$_4$Clx, 8.[9a] A 4.25 g (6.00 mmol) amount of **7** and 1.08 mL (13.35 mmol) of pyridine were dissolved in 25 mL of THF in a 50 mL round-bottom flask. A 2.28 mL (12.06 mmol) volume of $ClPPh_2$ was added slowly via a syringe. The mixture was stirred at 22 °C for 12 h, and the white precipitate formed was filtered out. The filtrate was evaporated to dryness by vacuum. The resulting residue was recrystallized from benzene, washed with 10 × 2 mL of Et_2O, and then dried by vacuum. A 67% yield (4.3 g) of colorless microcrystals of **8** was obtained. X-ray-quality crystals were obtained upon slow evaporation of a benzene solution of **8**. Details of the crystallographic analysis are provided below. ^{1}H NMR (δ, ppm; C_6D_6): 7.65 (m, 8H, PArH), 7.14−7.07 (m, 12 H, PArH), 6.94 (s, 4H), 6.59 (s, 6H), 4.74 (d, $^3J_{HP}$ = 10.1 Hz, 4H, $ArCH_2OP$), 4.53 (d, $^2J_{HH}$ = 13.2 Hz, 4H, $ArCH_2Ar$), 3.98 (t, $^3J_{HH}$ = 7.1 Hz, 4H, $ArOCH_2$), 3.79 (t, $^3J_{HH}$ = 7.1 Hz, 4H, $ArOCH_2$), 3.13 (d, $^2J_{HH}$ = 13.2 Hz, 4H, $ArCH_2Ar$), 1.94 (quint, $^3J_{HH}$ = 7.1 Hz, 4H, OCH_2CH_2Et), 1.85 (quint, $^3J_{HH}$ = 7.1 Hz, 4H, OCH_2CH_2Et), 1.41 (hex, $^3J_{HH}$ = 7.1 Hz, 4H, $O(CH_2)_2CH_2Me$), 1.35 (hex, $^3J_{HH}$ = 7.1 Hz, 4H, $O(CH_2)_2CH_2Me$), 0.98 (t, $^3J_{HH}$ = 7.1 Hz, 6H, CH_3), 0.97 (t, $^3J_{HH}$ = 7.1 Hz, 6H, CH_3). ^{13}C NMR (δ, ppm; C_6D_6): 157.2, 156.4, 143.1 (d, J_{CP} = 19 Hz), 136.0, 134.5, 132.8 (d, J_{CP} = 7.2 Hz), 130.9 (d, J_{CP} = 21 Hz), 129.3, 128.6, 128.4$_9$, 128.4$_7$, 122.7. ^{31}P NMR (δ, ppm; C_6D_6): 113.8 (s). MS (FAB; *m*/*z*): MH^+ = 1077.5. Anal.. Found for crystalline material: C, 77.93; H, 7.37. Calcd for $C_{70}H_{78}O_6P_2$ (M_r = 1077.31): C, 78.04; H, 7.30.

5,17-Bis((diphenylphosphino)methyl)-25,26,27,28-tetra-*n*-butoxycalix[4]arene, $(PPh_2CH_2)_2$-^{n}Bu$_4$Clx, 10.[9a,b] To a stirred solution of Ph_2PH (8.05 mmol) in 15 mL of dry THF at −78 °C was added 5.04 mL of 1.6 M ^{n}BuLi/hexane solution (8.06 mmol). The solution was stirred for 15 min at −78 °C and then transferred via a cannula to a solution of **9** (4.02 mmol) in 20 mL of dry THF at −78 °C. The mixture was stirred at −78 °C for 2 h and allowed to slowly warm to room temperature. The solution was stirred at room temperature for 12 h where the mixture was passed through a bed of Celite and then washed with toluene. The combined solution was reduced under vacuo. The oily residue was treated with hexane. The resultant white powder was recrystallized from a hexane solution at −30 °C. The colorless microcrystalline material

(44) Poli, R.; Krueger, S. T.; Mattamana, S. P. *Inorg. Synth.* **1998**, *32*, 200−201.
(45) Anderson, G. K.; Lin, M. *Inorg. Synth.* **1990**, *28*, 60−61.

formed was collected and vacuum-dried at 80 °C. This yielded 1.9 g of **10** in 45% yield. Crystals suitable for X-ray crystallographic analysis were obtained upon slow evaporation of a solution of **10** in benzene. Details of the crystallographic analysis are provided in the Supporting Information. ^{1}H NMR (δ, ppm; in C_6D_6): 7.49 (m, 8H, PArH), 7.13 (m, 12H, PArH), 6.91 (s, 4H, ArH), 6.52 (t, 2H, ArH), 6.35 (d, 4H, ArH), 4.51 (d, $^2J_{HH}$ = 13.2 Hz, 4H, $ArCH_2Ar$), 4.04 and 3.69 (t, $^3J_{HH}$ = 7.1 Hz, 8H, $ArOCH_2$), 3.34 (s, 4H, $ArCH_2P$), 3.10 (d, $^2J_{HH}$ = 13.2 Hz, 4H, $ArCH_2Ar$), 1.98 and 1.79 (m, 8H, OCH_2CH_2Et), 1.46 and 1.30 (m, 8H, $O(CH_2)_2CH_2Me$), 0.95 (m, 12H, CH_3). ^{31}P NMR (δ, ppm; in C_6D_6): −9.92 (s). MS (FAB; *m*/*z*): MH^+ = 1045.5. Anal. Found for crystalline material: C, 80.62; H, 7.58. Calcd for $C_{70}H_{78}O_4P_2$ (M_r = 1045.31): C, 80.43; H, 7.52.

CpTiMe[$(OCH_2)_2$-25,26,27,28-tetra-*n*-butoxycalix[4]-arene], CpTiMe[$(OCH_2)_2$-^{n}Bu_4Clx], 11. A 79.0 mg (0.5 mmol) amount of $CpTiMe_3$ was added to a solution of 354.5 mg (0.5 mmol) of **7**, in 5 mL of dry toluene. The solution was stirred at room temperature for 30 min. The volatile solvents were removed by vacuum. A pale yellow oil was produced, which when repeatedly washed with hexanes, and dried under vacuo, yielded an off-white powder in 97% yield. ^{1}H NMR (δ, ppm; C_6D_6): 7.14 (d, $^3J_{HH}$ = 7.6 Hz, 2H, A and C rings, *meta*-ArH), 7.13 (d, $^3J_{HH}$ = 7.6 Hz, 2H, A and C rings, *meta*-ArH), 7.01 (t, $^3J_{HH}$ = 7.6 Hz, 1H, A and C rings, *para*-ArH), 6.95 (t, $^3J_{HH}$ = 7.6 Hz, 1H, A and C rings, *para*-ArH), 6.445 (d, $^4J_{HH}$ = 2.2 Hz, 2H, B and D rings, *m*-ArH), 6.405 (d, $^4J_{HH}$ = 2.2 Hz, B and D rings, *m*-ArH), 6.03 (s, 5H, CpH), 4.90, 4.86 (AB-q, $^2J_{AB}$ = 12.5 Hz, 4H, $ArCH_2OTi$), 4.60 (d, $^2J_{HH}$ = 13 Hz, 2H, $ArCH_2Ar$), 4.57 (d, $^2J_{HH}$ = 13 Hz, 2H, $ArCH_2Ar$), 4.25 (t, $^3J_{HH}$ = 7.2 Hz, 2H, $ArOCH_2$), 4.22 (t, $^3J_{HH}$ = 7.2 Hz, 2H, $ArOCH_2$), 3.63 (t, $^3J_{HH}$ = 7.1 Hz, 4H, $ArOCH_2$), 3.21 (d, $^2J_{HH}$ = 13.2 Hz, 2H, $ArCH_2Ar$), 3.16 (d, $^2J_{HH}$ = 13.2 Hz, 2H, $ArCH_2Ar$), 2.10 and 1.79 (m, 8H, OCH_2CH_2Et), 1.51 and 1.26 (m, 8H, $O(CH_2)_2CH_2Me$), 1.00 (t, $^3J_{HH}$ = 7.1 Hz, 12H, CH_3), 0.8 (s, 3H, TiMe). High-resolution ESI-MS (positive-ion, CH_2Cl_2): calcd for **11** − CH_3^+, 819.4104 amu; obsd, 819.4115 amu (1.3 ppm). We were unable to obtain satisfactory elemental analysis.

{**cis-Cl_2Pd[$(PPh_2OCH_2)_2$-25,26,27,28-tetra-*n*-butoxycalix[4]-arene]}, cis-Cl_2Pd[$(PPh_2OCH_2)_2$-^{n}Bu_4Clx], 12.** A 0.108 g (0.10 mmol) amount of **8** and 0.038 g (0.10 mmol) of $Cl_2Pd(PhCN)_2$ were dissolved in 5 mL of benzene in a 20 mL round-bottom flask. The solution was gently refluxed for 45 min. After cooling, the volatile solvents were removed by vacuum. The residue was recrystallized from a solution mixture of 1:4 CH_2Cl_2/toluene. The pale yellow crystals that formed were collected, washed with 4 × 0.5 mL of hexane and 2 × 0.5 mL of Et_2O, and dried by vacuum. An 85% yield (0.11 g) of **12** was obtained. X-ray-quality crystals were obtained upon slow evaporation of $CHCl_3$/hexane solutions of **12**. Allowing the mother liquor to evaporate resulted in loss of crystallinity and is a result of the large number of chloroform solvates present in the lattice. ^{1}H NMR (δ, ppm; C_6D_6): 8.29 (m, 6H), 7.25−7.09 (m, 20H), 6.04 (s, 4H, ArH), 4.49 (d, $^2J_{HH}$ = 13.7 Hz, 4H, $ArCH_2Ar$), 4.15 (m, 4H, $ArOCH_2$), 4.0 (s, 4H, $ArCH_2$-OP), 3.53 (m, 4H, $ArOCH_2$), 2.99 (d, $^2J_{HH}$ = 13.7 Hz, 4H, $ArCH_2$-Ar), 1.93 (m, 4H, OCH_2CH_2Et), 1.70 (m, 4H, OCH_2CH_2Et), 1.50 (m, 4H, $O(CH_2)_2CH_2Me$), 1.19 (m, 4H, 4H, $O(CH_2)_2CH_2Me$), 0.94 (t, $^3J_{HH}$ = 7.2 Hz, 6H, CH_3), 0.93 (t, $^3J_{HH}$ = 7.1 Hz, 6H, CH_3), 0.11 (s, 3H, CH_3CN). ^{13}C NMR (δ, ppm; C_6D_6): calix-ArC, 158.2, 155.3, 137.1, 133.6, 133.2, 132.9, 129.1, 129.0, 128.2$_2$, 128.1$_5$, 125.3, 122.5; P−ArC, 133.5 (t, J_{CP} = 6.2 Hz), 132.9 (t, J_{CP} = 9.2 Hz), 131.8, 129.9 (t, J_{CP} = 4.1 Hz), 128.5 (t, J_{CP} = 5.1 Hz); calix-$ArCH_2Ar$, 74.7, 67.7; calix-ArO-^{n}Bu, 32.5, 32.4, 31.9, 31.3, 19.6, 19.0, 14.0, 13.8. ^{31}P NMR (δ, ppm; C_6D_6): 112.48 (s). High-resolution ESI-MS (postive-ion mode, CH_2Cl_2): calcd for **12** − Cl−, 1217.3997 amu; obsd, 1217.3973 amu (2.0 ppm). High-resolution ESI-MS (negative-ion mode): calcd for **12** + Cl^-, 1289.3378 amu; obsd, 1289.3362 amu (1.2 ppm). Crystalline samples failed to give adequate elemental analysis results, presumably due to the volatility of the $CHCl_3$ in the lattice. Batches of single crystals heated under vacuo (80 °C, 36 h, 5 mTorr) resulted in a loss of crystallinity but provided agreement with theory. Anal. Found: C, 67.18; H, 6.31. Calcd for $C_{70}H_{78}O_6P_2Cl_2Pd$ (M_r = 1254.63): C, 67.01; H, 6.27.

Bis(*μ*-chloro)bis[hydrogenbis(diphenylphosphinito)(1−)-P,P′]-dipalladium(II), *μ*-$Cl_2$$(PPh_2OH)_2$$(PPh_2O)_2$$Pd_2$, 13. A 0.100 g amount of **12** (79.7 *μ*mol) was dissolved in 10 mL of CH_2Cl_2 with vigorous stirring. Anhydrous HCl was passed through the solution for a period of 4 h. The solvent was removed under vacuo, and the resultant residue was triturated with hexanes. The hexane precipitate was collected by filtration and recrystallized from $CHCl_3$/hexane (7:3), where the solid was dried under vacuo providing an isolated yield of **13** in 91%. ^{1}H NMR (δ, ppm; in $CDCl_3$): 8.03 (br s, 2H, O*H*), 7.902 (m, 16H, *m*-*H*), 7.058 (m, *p*-*H*), 7.011 (m, *o*-*H*); both resonances at 7.058 and 7.011 integrate to 24 H. ^{31}P NMR (δ, ppm; in $CDCl_3$): 77.91 (s); cf. previously obtained value of 78.1 ppm that was obtained in the same solvent.[22] The hexane washes were found to contain **9** and some trace unidentified products. Elemental analysis was consistent with solid material containing **13**·$CHCl_3$. Anal. Calcd (found): C, 48.64 (48.74); H, 3.58 (3.60).

{***fac*-$(CO)_3$Mo$(NCCH_3)$[$(PPh_2OCH_2)_2$-25,26,27,28-tetra-*n*-butoxycalix[4]arene]}, *fac*-$(CO)_3$Mo$(NCCH_3)$[$(PPh_2OCH_2)_2$-^{n}Bu_4Clx], 14a. A** 1.08 g (1.00 mmol) amount of **8** and 0.272 g (1.00 mmol) of $Mo(CO)_3$(toluene) were dissolved in 40 mL of MeCN in a 50 mL round-bottom flask. The mixture was gently refluxed for 3 h. After cooling, the mixture was filtered, washed with 2 × 1 mL of MeCN and 2 × 1 mL of Et_2O, and dried by vacuum. An 86% yield (1.1 g) of pale yellow crystals of **14a** was obtained. No crystals of X-ray quality were obtained despite repeated attempts. IR (ν_{CO}, cm^{-1}, KBr): 1942 (s), 1846 (s), 1832 (s). ^{1}H NMR (δ, ppm; $CDCl_3$): 8.14 (m, 3H, ArH), 7.98 (m, 3H, Ar−H), 7.30−6.99 (m, 20 H, PC_6H_5), 6.495 (d, $^4J_{HH}$ = 1.5 Hz, 2H, B and D rings, *m*-ArH), 6.459 (d, $^4J_{HH}$ = 1.5 Hz, B and D rings, *m*-ArH), 4.63 (d, $^2J_{HH}$ = 13.4 Hz, 2H, $ArCH_2Ar$), 4.59$_5$ (d, $^2J_{HH}$ = 13.4 Hz, 2H, $ArCH_2Ar$), 4.43 (AB q, $^2J_{HH}$ = 11.1 Hz, 4H, $ArCH_2OP$), 4.25 (m, 4H, $ArOCH_2$), 3.60 (m, 4H, $ArOCH_2$), 3.181 (d, $^2J_{HH}$ = 13.4 Hz, 2H, $ArCH_2Ar$), 3.171 (d, $^2J_{HH}$ = 13.4 Hz, 2H $ArCH_2Ar$), 2.04 (m, 4H, OCH_2CH_2Et), 1.75 (m, 4H, OCH_2CH_2-Et), 1.54 (m, 4H, $O(CH_2)_2CH_2Me$), 1.25 (m, 4H, 4H, $O(CH_2)_2CH_2$-Me), 0.98 (t, $^3J_{HH}$ = 7.1 Hz, 6H, CH_3), 0.96 (t, $^3J_{HH}$ = 7.1 Hz, 6H, CH_3), 0.11 (s, 3H, CH_3CN). ^{31}P NMR (δ, ppm; C_6D_6): 145.2 (s). High-resolution ESI-MS spectra of **14a** resulted in a signal intensity too low to observe in CH_2Cl_2. An adequate signal for (**14a** − CH_3CN + H^+) was observed in CH_2Cl_2/MeOH (9:1) with an observed mass of 1259.4271 amu (1.6 ppm). Platelike crystals (25 °C, 5 d, 5 mTorr) sealed in an ampule under nitrogen provided the sample for elemental analysis. Anal. Found: C, 69.28; H, 6.26; N, 1.07. Calcd for $C_{75}H_{81}NO_9P_2Mo$ (M_r = 1298.33): C, 69.38; H, 6.29; N, 1.08.

{***fac*-$(CO)_3$Mo$(NCCH_2CH_3)$[$(PPh_2OCH_2)_2$-25,26,27,28-tetra-*n*-butoxycalix[4]arene]}, *fac*-$(CO)_3$Mo$(NCCH_2CH_3)$[$(PPh_2OCH_2)_2$-^{n}Bu_4Clx], 14b.** A 0.54 g (0.50 mmol) amount of **8** and 0.14 g (0.50 mmol) of $Mo(CO)_3$(toluene) were dissolved in 5 mL of EtCN in a 25 mL round-bottom flask. The mixture was stirred at 22 °C for 24 h. The pale yellow crystals that formed were collected, washed with 2 × 1 mL of EtCN and 2 × 1 mL of Et_2O, and vacuum-dried. A 64% yield (0.42 g) of **14b** was obtained. We were able to

collect data on crystals of **14b**, but the crystal quality was very poor giving rise to an incomplete solution. The data obtained were good enough to determine the coordination sphere about the molybdenum; see Figure S12. IR (ν_{CO}, cm^{-1}, KBr): 1943 (s), 1859 (s), 1833 (s). ^1H NMR (δ, ppm; $CDCl_3$): 8.15 (m, 3H, ArH), 8.00 (m, 3H, ArH), 7.30−7.00 (m, 20 H, PC_6H_5), 6.500 (d, $^4J_{HH}$ = 1.6 Hz, B and D ring *m*-ArH, 2H), 6.459 (d, $^4J_{HH}$ = 1.6 Hz, B and D ring *m*-ArH, 2H), 4.627 (d, $^2J_{HH}$ = 13.7 Hz, $ArCH_2Ar$, 2H), 4.595 (d, $^2J_{HH}$ = 13.7 Hz, $ArCH_2Ar$, 2H), 4.472, 4.372 (AB q, $^2J_{HH}$ = 11.6 Hz, $ArCH_2OP$, 4H), 4.24 (m, 4H, $ArOCH_2$), 3.60 (m, 4H, $ArOCH_2$), 3.179 (d, $^2J_{HH}$ = 13.7 Hz, $ArCH_2Ar$, 2H), 3.163 (d, $^2J_{HH}$ = 13.7 Hz, $ArCH_2Ar$, 2H), 2.03 (m, 4H, OCH_2CH_2Et), 1.75 (m, 4H, OCH_2CH_2Et), 1.54 (m, 4H, $O(CH_2)_2CH_2Me$), 1.25 (m, 4H, 4H, $O(CH_2)_2CH_2Me$), 0.97 (t, $^3J_{HH}$ = 7.1 Hz, 6H, CH_3), 0.96 (t, $^3J_{HH}$ = 7.1 Hz, 6H, CH_3), 0.72 (q, $^3J_{HH}$ = 7.2 Hz, 2H, $MeCH_2$-CN), −0.15 (t, $^3J_{HH}$ = 7.2 Hz, 3H, CH_3CH_2CN). ^{31}P NMR (δ, ppm; C_6D_6): 145.0 (s). High-resolution ESI-MS of **14b** experienced the same problem as in **14a**. There was an observed mass of 1259.4276 amu for (**14b** $-CH_3CH_2CN + H^+$) in CH_2Cl_2/MeOH (9:1) (1.8 ppm). Platelike crystals (25 °C, 5 d, 5 mTorr) sealed in an ampule under nitrogen provided a sample for elemental analysis. Anal. Found: C, 69.60; H, 6.40; N, 1.07. Calcd for $C_{76}H_{83}NO_9P_2Mo$ (M_r = 1312.36): C, 69.56; H, 6.38; N, 1.07.

{Mo(CO)$_4$[(PPh$_2$OCH$_2$)$_2$-25,26,27,28-tetra-*n*-butoxycalix[4]-arene]}, Mo(CO)$_4$(PPh$_2$OCH$_2$)$_2$-^{n}Bu$_4$Clx), 14c. A 100.0 mg (0.077 mmol) amount of **14a** was dissolved in 15 mL of benzene in a 50 mL round-bottom flask equipped with a sidearm. The solution was purged slowly with CO at 22 °C for 20 h, and the volatile reagents/solvents were removed by vacuum. A 98% yield (97 mg) of colorless **14c** was obtained. X-ray-quality crystals were grown from solutions of benzene/methylene chloride by slow evaporation at room temperature. Details of the crystallographic analysis are given below. IR (ν_{CO}, cm^{-1}, KBr): 2025 (w), 1931 (s), 1916 (s), 1905 (s). ^1H NMR (δ, ppm; C_6D_6): 7.90 (m, 6H, ArH), 7.25−7.03 (m, 20 H, PC_6H_5), 6.39 (s, 4H, ArH), 4.60 (d, $^2J_{HH}$ = 15.3 Hz, 4H, $ArCH_2Ar$), 4.35 (s, 4H, $ArCH_2OP$), 4.23 (m, 4H, $ArOCH_2$), 3.60 (m, 4H, $ArOCH_2$), 3.16 (d, $^2J_{HH}$ = 15.3 Hz, 4H, $ArCH_2Ar$), 2.04 (m, 4H, OCH_2CH_2Et), 1.76 (m, 4H, OCH_2CH_2Et), 1.55 (m, 4H, $O(CH_2)_2CH_2Me$), 1.25 (m, 4H, 4H, $O(CH_2)_2CH_2Me$), 0.99 (t, $^3J_{HH}$ = 7.1 Hz, 6H, CH_3), 0.98 (t, $^3J_{HH}$ = 7.1 Hz, 6H, CH_3). ^{13}C NMR (δ, ppm; C_6D_6): 216.2 (low intensity, unable to resolve coupling), 210.3 (vt, J_{CP} = 11 Hz), 158.6, 155.1, 141.5 (vt, J_{CP} = 19 Hz), 137.7, 133.3, 131.7 (vt, J_{CP} = 5 Hz), 131.2 (vt, J_{CP} = 7 Hz), 130.2, 129.2, 128.7 (vt, J_{CP} = 5 Hz), 128.5, 124.6, 122.8, 75.1_1, 75.0_5 65.7, 32.9, 32.4, 31.6, 20.0, 19.4, 14.4, 14.2. ^{31}P NMR (δ, ppm; in C_6D_6): 145.2 (s). High-resolution ESI-MS of **14c** experienced the same problem as in **14a**. There was an observed mass of 1287.4210 amu for (**14c** + H^+) in CH_2Cl_2/MeOH (9:1) (0.6 ppm). Crystalline material subjected to evacuation (70 °C, 3d, 5 mTorr) resulted in the observed elemental analysis. Anal. Found: C, 69.41; H, 6.14. Calcd for $C_{74}H_{78}O_{10}P_2Mo$ (M_r = 1285.29): C, 69.15; H, 6.12.

***fac*-Tris(carbonyl)(NCCH$_3$)[(PPh$_2$CH$_2$)$_2$-^{n}Bu$_4$Clx]molybdenum(0), *fac*-(CO)$_3$Mo(NCCH$_3$)[(PPh$_2$CH$_2$)$_2$-^{n}Bu$_4$Clx], 17.** A 104.5 mg (0.10 mmol) amount of {$(CH_2PPh_2)_2$-^{n}Bu$_4$Clx}, **10**, and a 28.4 mg (0.10 mmol) amount of $Mo(CO)_3$(toluene) were dissolved in 15 mL of acetonitrile in a 50 mL round-bottom flask. The mixture was heated to gentle reflux for 24 h. After cooling, the volatiles were removed in a vacuum and the residue was extracted with Et_2O. The Et_2O was removed under reduced pressure, and the residue was redissolved in benzene-d_6. Analysis by ^1H NMR showed the reaction to be incomplete. The sample was returned to the flask and, upon removal of volatiles, was resuspended in 15 mL of acetonitrile, where the solution was refluxed for another 4 days. Analysis by ^1H NMR showed the reaction to be incomplete even after this extended period of time. IR (ν_{CO}, cm^{-1}, KBr): cis 2039 (w), 1952 (m), 1896 (vs), 1869 (s); additional peak found in ν_{CO} region 2001 (w). ^{31}P NMR (δ, ppm; C_6D_6): 28.5 (d, J = 28 Hz), 28.1 (d, J = 28 Hz).

Acknowledgment is made for the financial support provided by the Research Corporation for a Research Innovation Award, and through the Petroleum Research Fund, administered by the American Chemical Society.

Supporting Information Available: Experimental details for the synthesis of **1**−**6** and **9**, comparison ^1H NMR spectra of **7** and **11**, **8** and **12**, and **8**, **14a**, **14b,** and **14c**, ORTEP representations for **3**−**8**, **10**, **13**, and **14b**, and complete crystallographic data available as a CIF file. This material is available free of charge via the Internet at http://pubs.acs.org.

IC020446B